[26] Kunikata T, Yamane H, Segi E, *et al.* Suppression of allergic inflammation by the prostaglandin E receptor subtype EP3. Nat Immunol 2005; 6: 524-31.

[27] Schratl P, Royer JF, Kostenis E, *et al.* The role of the prostaglandin D2 receptor, DP, in eosinophil trafficking. J Immunol 2007; 179: 4792-9.

[28] Mita H, Hasegawa M, Higashi N, Akiyama K. Characterization of PGE2 receptor subtypes in human eosinophils. J Allergy Clin Immunol 2002; 110: 457-9.

[29] Peacock CD, Misso NL, Watkins DN, Thompson PJ. PGE 2 and dibutyryl cyclic adenosine monophosphate prolong eosinophil survival *in vitro*. J Allergy Clin Immunol 1999; 104: 153-62.

[30] Yamane H, Sugimoto Y, Tanaka S, Ichikawa A. Prostaglandin E(2) receptors, EP2 and EP4, differentially modulate TNF-alpha and IL-6 production induced by lipopolysaccharide in mouse peritoneal neutrophils. Biochem Biophys Res Commun 2000; 278: 224-8.

[31] Kabashima K, Miyachi Y. Prostanoids in the cutaneous immune response. J Dermatol Sci 2004; 34: 177-84.

[32] Youn CS, Cho KH. Eosinophilic pustular folliculitis treated with naproxen. Br J Dermatol 2001; 145: 514-5.

[33] Wong RC, Kang S, Heezen JL, Voorhees JJ, Ellis CN. Oral ibuprofen and tetracycline for the treatment of acne vulgaris. J Am Acad Dermatol 1984; 11: 1076-81.

[34] Becker D, Knop J. Mechanism in allergic contact dermatitis. Exp Dermatol 1993; 2: 63-9.

[35] Grabbe S, Schwarz T. Immunoregulatory mechanisms involved in elicitation of allergic contact hypersensitivity. Immunol Today 1998; 19: 37-44.

[36] Angeli V, Staumont D, Charbonnier AS, *et al.* Activation of the D prostanoid receptor 1 regulates immune and skin allergic responses. J Immunol 2004; 172: 3822-9.

[37] Hammad H, Kool M, Soullie T, *et al.* Activation of the D prostanoid 1 receptor suppresses asthma by modulation of lung dendritic cell function and induction of regulatory T cells. J Exp Med 2007; 204: 357-67.

[38] Zhou W, Hashimoto K, Goleniewska K, *et al.* Prostaglandin i2 analogs inhibit proinflammatory cytokine production and T cell stimulatory function of dendritic cells. J Immunol 2007; 178: 702-10.

[39] Robbiani DF, Finch RA, Jager D, Muller WA, Sartorelli AC, Randolph GJ. The leukotriene C(4) transporter MRP1 regulates CCL19 (MIP-3beta, ELC)-dependent mobilization of dendritic cells to lymph nodes. Cell 2000; 103: 757-68.

[40] Nakae S, Komiyama Y, Nambu A, *et al.* Antigen-specific T cell sensitization is impaired in IL-17-deficient mice, causing suppression of allergic cellular and humoral responses. Immunity 2002; 17: 375-87.

[41] Nagamachi M, Sakata D, Kabashima K, *et al.* Facilitation of Th1-mediated immune response by prostaglandin E receptor EP1. J Exp Med 2007; 204: 2865-74.

[42] Nakajima S, Honda T, Sakata D, *et al.* Prostaglandin I2-IP signaling promotes Th1 differentiation in a mouse model of contact hypersensitivity. J Immunol 2010; 184(10): 5595-603.

[43] Sakaguchi S, Yamaguchi T, Nomura T, Ono M. Regulatory T cells and immune tolerance. Cell 2008; 133: 775-87.

[44] Honda T, Miyachi Y, Kabashima K. The Role of Regulatory T Cells in Contact Hypersensitivity. Recent Pat Inflamm Allergy Drug Discov 2010; 4(2): 85-9

[45] Tomura M, Honda T, Tanizaki H, *et al.* Activated regulatory T cells are the major T cell type emigrating from the skin during a cutaneous immune response in mice. J Clin Invest 2010; 120(3): 883-93.

[46] Sharma S, Yang SC, Zhu L, *et al.* Tumor cyclooxygenase-2/prostaglandin E2-dependent promotion of FOXP3 expression and CD4+ CD25+ T regulatory cell activities in lung cancer. Cancer Res 2005; 65: 5211-20.

[47] Homey B, Alenius H, Muller A, *et al.* CCL27-CCR10 interactions regulate T cell-mediated skin inflammation. Nat Med 2002; 8: 157-65.

[48] Takeshita K, Yamasaki T, Nagao K, *et al.* CRTH2 is a prominent effector in contact hypersensitivity-induced neutrophil inflammation. Int Immunol 2004; 16: 947-59.

[49] Boehme SA, Chen EP, Franz-Bacon K, *et al.* Antagonism of CRTH2 ameliorates chronic epicutaneous sensitization-induced inflammation by multiple mechanisms. Int Immunol 2009; 21: 1-17.

[50] Honda T, Matsuoka T, Ueta M, Kabashima K, Miyachi Y, Narumiya S. Prostaglandin E(2)-EP(3) signaling suppresses skin inflammation in murine contact hypersensitivity. J Allergy Clin Immunol 2009; 124: 809-18 e802.

[51] Murakawa M, Yamaoka K, Tanaka Y, Fukuda, Y. Involvement of tumor necrosis factor (TNF)-alpha in phorbol ester 12-O-tetradecanoylphorbol-13-acetate (TPA)-induced skin edema in mice. Biochem Pharmacol 2006; 71: 1331-6.

[52] Flower RJ, Harvey EA, Kingston WP. Inflammatory effects of prostaglandin D2 in rat and human skin. Br J Pharmacol 1976; 56: 229-33.

[53] Crunkhorn P, Willis AL. Cutaneous reactions to intradermal prostaglandins. Br J Pharmacol 1971; 41: 49-56.

[54] Basran GS, Morley J, Paul W, Turner-Warwick M. Evidence in man of synergistic interaction between putative mediators of acute inflammation and asthma. Lancet 1982; 1: 935-37.

[55] Kabashima K, Nagamachi M, Honda T, *et al.* Prostaglandin E(2) is required for ultraviolet B-induced skin inflammation via EP2 and EP4 receptors. Lab Invest 2007; 87: 49-55.

[56] Kawashima M, Harada S. Effect of standard medication on quality of life of patients with atopic dermatitis. J Dermatol 2007; 34: 9-16.

[57] Kawashima M, Tango T, Noguchi T, Inagi M, Nakagawa H, Harada S. Addition of fexofenadine to a topical corticosteroid reduces the pruritus associated with atopic dermatitis in a 1-week randomized, multicentre, double-blind, placebo-controlled, parallel-group study. Br J Dermatol 2007; 148: 1212-21.

[58] Fogh K, Herlin T, Kragballe K. Eicosanoids in skin of patients with atopic dermatitis: prostaglandin E2 and leukotriene B4 are present in biologically active concentrations. J Allergy Clin Immunol 1989; 83: 450-5.

[59] Archer CB, Page CP, Juhlin L, Morley J, MacDonald DM. Delayed-onset synergism between leukotriene B4 and prostaglandin E2 in human skin. Prostaglandins 1987; 33: 799-805.

[60] Archer CB, Frohlich W, Page CW, Paul W, Morley J, MacDonald DM. Synergistic interaction between prostaglandins and PAF-acether in experimental animals and man. Prostaglandins 1984; 27: 495-501.

[61] Lee CH, Chuang HY, Shih CC, Jong SB, Chang CH, Yu HS. Transepidermal water loss, serum IgE and beta-endorphin as important and independent biological markers for development of itch intensity in atopic dermatitis. Br J Dermatol 2006; 154: 1100-7.

[62] Hirai H, Tanaka K, Yoshie O, *et al.* Prostaglandin D2 selectively induces chemotaxis in T helper type 2 cells, eosinophils, and basophils via seven-transmembrane receptor CRTH2. J Exp Med 2001; 193: 255-61.

[63] Yoshimura-Uchiyama C, Iikura M, Yamaguchi M, *et al.* Differential modulation of human basophil functions through prostaglandin D2 receptors DP and chemoattractant receptor-homologous molecule expressed on Th2 cells/DP2. Clin Exp Allergy 2004; 34: 1283-90.

[64] Iwasaki M, Nagata K, Takano S, Takahashi K, Ishii N, Ikezawa Z. Association of a new-type prostaglandin D2 receptor CRTH2 with circulating T helper 2 cells in patients with atopic dermatitis. J Invest Dermatol 2002; 119: 609-16.

[65] Neisius U, Olsson R, Rukwied R, Lischetzki G, Schmelz M. Prostaglandin E2 induces vasodilation and pruritus, but no protein extravasation in atopic dermatitis and controls. J Am Acad Dermatol 2002; 47: 28-32.

[66] Arai I, Takano N, Hashimoto Y, *et al.* Prostanoid DP1 receptor agonist inhibits the pruritic activity in NC/Nga mice with atopic dermatitis. Eur J Pharmacol 2004; 505: 229-35.

[67] Matsuoka T, Hirata M, Tanaka H, *et al.* Prostaglandin D2 as a mediator of allergic asthma. Science 2000; 287: 2013-7.

[68] Robinson C, Hardy CC, Holgate ST. Pulmonary synthesis, release, and metabolism of prostaglandins. J Allergy Clin Immunol 1985; 76: 265-71.

[69] Herrerias A, Torres R, Serra M, *et al.* Activity of the cyclooxygenase 2-prostaglandin-E prostanoid receptor pathway in mice exposed to house dust mite aeroallergens, and impact of exogenous prostaglandin E2. J Inflamm (Lond) 2009; 6: 30.

[70] Zhao Y, Tong J, He D, *et al.* Role of lysophosphatidic acid receptor LPA2 in the development of allergic airway inflammation in a murine model of asthma. Respir Res 2009; 10: 114.

[71] Oguma T, Palmer LJ, Birben E, Sonna LA, Asano K, Lilly CM. Role of prostanoid DP receptor variants in susceptibility to asthma. N Engl J Med 2004; 351: 1752-63.

[72] Uller L, Mathiesen JM, Alenmyr L, *et al.* Antagonism of the prostaglandin D2 receptor CRTH2 attenuates asthma pathology in mouse eosinophilic airway inflammation. Respir Res 2007; 8: 16.

[73] Spik I, Brenuchon C, Angeli V, *et al.* Activation of the prostaglandin D2 receptor DP2/CRTH2 increases allergic inflammation in mouse. J Immunol 2005; 174: 3703-8.

[74] Chevalier E, Stock J, Fisher T, *et al.* Cutting edge: chemoattractant receptor-homologous molecule expressed on Th2 cells plays a restricting role on IL-5 production and eosinophil recruitment. J Immunol 2005; 175: 2056-60.

[75] Ueta M, Matsuoka T, Narumiya S, Kinoshita S. Prostaglandin E receptor subtype EP3 in conjunctival epithelium regulates late-phase reaction of experimental allergic conjunctivitis. J Allergy Clin Immunol 2009; 123: 466-71.

[76] Kamei D, Yamakawa K, Takegoshi Y, *et al.* Reduced pain hypersensitivity and inflammation in mice lacking microsomal prostaglandin e synthase-1. J Biol Chem 2004; 279: 33684-95.

[77] McCoy JM, Wicks JR, Audoly LP. The role of prostaglandin E2 receptors in the pathogenesis of rheumatoid arthritis. J Clin Invest 2002; 110: 651-8.

[78] Honda T, Segi-Nishida E, Miyachi Y, Narumiya S. Prostacyclin-IP signaling and prostaglandin E2-EP2/EP4 signaling both mediate joint inflammation in mouse collagen-induced arthritis. J Exp Med 2006; 203: 325-35.

[79] Yao C, Sakata D, Esaki Y, *et al.* Prostaglandin E2-EP4 signaling promotes immune inflammation through Th1 cell differentiation and Th17 cell expansion. Nat Med 2009; 15: 633-40.

Received: December 30, 2009 Revised: July 15, 2010 Accepted: August 04, 2010

The American Journal of Pathology, Vol. 176, No. 5, May 2010

DOI: 10.2353/ajpath.2010.090957

Molecular Pathogenesis of Genetic and Inherited Diseases

Flaky Tail Mouse Denotes Human Atopic Dermatitis in the Steady State and by Topical Application with *Dermatophagoides pteronyssinus* Extract

Catharina Sagita Moniaga,* Gyohei Egawa,*† Hiroshi Kawasaki,‡ Mariko Hara-Chikuma,* Tetsuya Honda,* Hideaki Tanizaki,* Saeko Nakajima,* Atsushi Otsuka,* Hiroyuki Matsuoka,§ Akiharu Kubo,‡ Jun-ichi Sakabe,¶ Yoshiki Tokura,¶ Yoshiki Miyachi,* Masayuki Amagai,‡ and Kenji Kabashima*†

From the Department of Dermatology, and the Center for Innovation in Immunoregulative Technology and Therapeutics,† Graduate School of Medicine, Kyoto University, Kyoto; the Department of Dermatology,‡ Faculty of Medicine, Keio University, Tokyo; the Division of Medical Zoology,§ Jichi Medical University, Tochigi-ken; and the Department of Dermatology,¶ University of Occupational and Environmental Health, Fukuoka, Japan*

The barrier abnormality, a loss-of-function mutation in the gene encoding filaggrin (*FLG*), which is linked to the incidence of atopic dermatitis (AD), is a recently discovered but important factor in the pathogenesis of AD. Flaky tail (*Flg^{ft}*) mice, essentially deficient in filaggrin, have been used to investigate the role of filaggrin on AD. However, the relevancy of *Flg^{ft}* mice to human AD needs to be determined further. In this study, we observed the clinical manifestations of *Flg^{ft}* mice in the steady state and their cutaneous immune responses against external stimuli, favoring human AD. Under specific pathogen-free conditions, the majority of *Flg^{ft}* mice developed clinical and histological eczematous skin lesions similar to human AD with outside-to-inside skin barrier dysfunction evaluated by newly devised methods. In addition, cutaneous hapten-induced contact hypersensitivity as a model of acquired immune response and a mite extract-induced dermatitis model physiologically relevant to a human AD were enhanced in *Flg^{ft}* mice. These results suggest that the *Flg^{ft}* mouse genotype has potential as an animal model of AD corresponding with filaggrin mutation in human AD. *(Am J Pathol 2010, 176:2385–2393; DOI: 10.2353/ajpath.2010.090957)*

Atopic dermatitis (AD), which affects at least 15% of children in developed countries, is characterized by eczematous skin lesions, dry skin, and pruritus.[1–3] Although the precise pathogenic mechanism of AD is as yet unknown, several accumulated lines of evidence suggest that a defective skin barrier to environmental stimuli may contribute to its pathogenesis. It has long been thought that the barrier abnormality in AD is not merely an epiphenomenon but rather is the "driver" of disease activity.[4] The evidence for a primary structural abnormality of the stratum corneum in AD is derived from a recently discovered link between the incidence of AD and loss-of-function mutations in the gene encoding filaggrin (*FLG*). Individuals carrying the *FLG* null allele variants tend to develop AD.[5–7]

Filaggrin protein is localized in the granular layers of the epidermis. Profilaggrin, a 400-kDa polyprotein, is the main component of keratohyalin granules.[8–10] In the differentiation of keratinocytes, profilaggrin is dephosphorylated and cleaved into 10 to 12 essentially identical 27-kDa filaggrin molecules, which aggregate in the keratin cytoskeleton system to form a dense protein-lipid matrix.[10] This structure is thought to prevent epidermal water loss and impede the entry of external stimuli, such as allergens, toxic chemicals, and infectious organisms. Therefore, filaggrin is a key protein in the terminal differentiation of the epidermis and in skin barrier function.[11]

Because AD is a common disease for which satisfactory therapies have not yet been established, understanding the mechanism of AD through animal models is an essential issue.[1,12] Flaky tail (*Flg^{ft}*) mice, first introduced in 1958, are spontaneously mutated mice with

Supported in part by the Ministry of Education, Culture, Sports, Science, and Technology of Japan and the Ministry of Health, Labor, and Welfare of Japan.

Accepted for publication January 11, 2010.

Supplemental material for this article can be found on *http://ajp.amjpathol.org*.

Address reprint requests to Dr. Kenji Kabashima, M.D., Ph.D., Department of Dermatology and Center for Innovation in Immunoregulative Technology and Therapeutics, Kyoto University Graduate School of Medicine, 54 Shogoin-Kawara, Kyoto 606-8507, Japan. E-mail: kaba@kuhp.kyoto-u.ac.jp.

abnormally small ears, tail constriction, and a flaky appearance of the tail skin, which is most evident between 5 and 14 days of age.[13] Mice of the *Flg*^{ft} genotype express an abnormal profilaggrin polypeptide that does not form normal keratohyalin F granules and is not proteolytically processed to filaggrin. Therefore, filaggrin is absent from the cornified layers in the epidermis of the *Flg*^{ft} mouse.[14–16]

Recently, it has been revealed that the gene responsible for the characteristic phenotype of *Flg*^{ft} mice is a nonsense mutation of 1-bp deletion analogous to a common human *FLG* mutation.[15] These mice developed eczematous skin lesions after age 28 weeks under specific pathogen-free (SPF) conditions[17] and enhanced penetration of tracer perfusion determined by ultrastructural visualization,[16] and were predisposed to develop an allergen-specific immune response after epicutaneous sensitization with the foreign allergen ovalbumin (OVA).[15,17] On the other hand, general immunity through intraperitoneal sensitization with OVA was comparable between *Flg*^{ft} mice and control mice.[15,17]

Despite these recent advances, there still remain several issues with *Flg*^{ft} mice to be addressed. For example, serial close observation of clinical manifestations in reference to human AD will be informative. It is of value to evaluate the responses to external stimuli relevant to human AD, such as mite extracts, instead of OVA that has been used previously. A comparative study on the skin-mediated contact hypersensitivity (CHS) response and non-skin-mediated delayed-type hypersensitivity response is important to evaluate the impact of barrier dysfunction on immune responses *in vivo*. In addition, although it has now been determined that the barrier dysfunction is a key element in the establishment of AD, there is no established method to evaluate the outside-to-inside barrier function quantitatively.

In this study, we found that *Flg*^{ft} mice showed spontaneous dermatitis with skin lesions mimicking human AD in a steady state under SPF conditions: serial occurrence of manifestations as scaling, erythema, pruritus, and erosion followed by edema in this order. We also successfully evaluated outside-to-inside barrier dysfunction in *Flg*^{ft} mice quantitatively using a newly developed method. In addition, we determined that the Th1/Tc1-mediated immune response was enhanced by immunization through skin but not through non-skin immunization. Last, we induced severe AD-like skin lesions in *Flg*^{ft} mice by application of mites as a physiologically relevant antigen for human AD, which will be an applicable animal model of AD.

Materials and Methods

Mice

C57BL/6NCrSlc (B6) mice were purchased from SLC (Shizuoka, Japan). Flaky tail (STOCK *a/a ma ft/ma ft*/J; *Flg*^{ft} mice) mice have double-homozygous filaggrin (*Flg*) and matted (*ma*) mutations.[13,14] We used B6 mice as a control of *Flg*^{ft} mice because *Flg*^{ft} mice were described to be outcrossed onto B6 mice at The Jackson Laboratory (Bar Harbor, ME)[13,14] (of note, although the strain was crossed with B6, it is not a B6 congenic strain but rather a hybrid stock that is probably semi-inbred). Female mice were used in all experiments unless otherwise stated; they were maintained on a 12-hour light/dark cycle at a temperature of 24°C and at a humidity of 50 + 10% under SPF conditions at Kyoto University Graduate School of Medicine. Routine colony surveillance and diagnostic workup verified that mice were free of Ectromelia virus, lymphocytic choriomeningitis virus, mouse hepatitis virus, Sendai virus, *Mycoplasma pulmonis*, cilia-associated respiratory bacillus, *Citrobacter rodentium* [*Escherichia coli* O115a,c:K(B)], *Clostridium piliforme* (Tyzzer's organism), *Corynebacterium kutscheri*, *Helicobacter hepaticus*, *Pasteurella pneumotropica*, *Salmonella* spp., parasites, intestinal protozoans, *Enterobius*, and ectoparasites. All experimental procedures were approved by the Institutional Animal Care and Use Committee of Kyoto University Graduate School of Medicine.

Clinical Observation and Histology

The clinical severity of skin lesions was scored according to the macroscopic diagnostic criteria that were used for the NC/Nga mouse.[18] In brief, the total clinical score for skin lesions was designated as the sum of individual scores, graded as 0 (none), 1 (mild), 2 (moderate), and 3 (severe), for the symptoms of pruritus, erythema, edema, erosion, and scaling. Pruritus was observed clinically for more than 2 minutes.

For the histological portion of the study, the dorsal skin of mice was stained with H&E. Toluidine blue staining was used to detect mast cells, and the number of mast cells was calculated as the average from five different fields of each sample ×40 magnification).

Flow Cytometric Analysis and Quantitative RT-PCR

Cells from the skin-draining axillary and inguinal lymph nodes (LNs) and from the spleen were analyzed with flow cytometry. Fluorescent-labeled anti-CD4 and anti-CD8 antibodies were obtained from eBioscience (San Diego, CA) and used to stain cells. The total number of cells per organ and the number of cells in each subset were calculated through flow cytometry using the FACSCanto II system (Becton Dickinson, San Diego, CA). Quantitative RT-PCR was performed as described previously, using the housekeeping gene glyceraldehyde-3-phosphate dehydrogenase (*GAPDH*) as a control.[19]

Total and Mite-Specific Serum IgE

Total serum IgE levels were measured with a mouse IgE ELISA Kit (Bethyl Laboratories, Montgomery, TX) according to the manufacturer's protocols. For the measurement of mite-specific IgE levels, the same type of mouse IgE ELISA Kit was used with slightly modifications. Specifi-

cally, plates were coated and incubated with 10 μg/ml *Dermatophagoides pteronyssinus* (Dp) (Biostir, Kobe, Japan) diluted with coating buffer for 60 minutes. After a blocking period of 30 minutes, 100 μl of 5× diluted serum was added into each well and incubated for 2 hours. Anti-mouse IgE-horseradish peroxidase conjugate (1:15,000; 100 μL) was used to conjugate the antigen-antibody complex for 60 minutes at room temperature; from this point on the ELISA Kit was used according to the manufacturer's protocol. Absorbance was measured at 450 nm. The difference between the sample absorbance and the mean of negative control absorbance was taken as the result.

Skin Barrier Function

The dorsal regions of the skin were shaved in all mice before measurement. To evaluate inside-to-outside barrier function, transepidermal water loss (TEWL) was measured with a Tewameter Vapo Scan (Asahi Biomed, Tokyo, Japan) at 24°C and 46% relative humidity.

Outside-to-inside barrier function was assessed by means of fluorescein isothiocyanate isomer I (FITC) (Sigma-Aldrich, St. Louis, MO). The shaved dorsal skin of mice was treated with 100 μl of 1% FITC diluted in acetone and dibutyl phthalate (1:4); 3 hours later, this area was tape-stripped (Scotch tape, 3M, St. Paul, MN) nine times to remove the stratum corneum containing the remnant of FITC. The painted area (1.2 cm × 1.2 cm) was removed, and FITC concentration was measured. Each skin sample was soaked in PBS at 60°C for 10 seconds, after which the dermis and epidermis were separated. The epidermis was soaked in 500 μl of PBS, homogenized, and spun down at 2200 × *g*. The supernatant was collected, and fluorescence was measured at an excitation wavelength of 535 nm and an emission wavelength of 460 nm using an Arvo SX 1420 counter (Wallac, PerkinElmer, Waltham, MA). The fluorescence value was compared with a standard curve using FITC serial dilutions.

For the evaluation of fluorescence intensities of FITC penetrated into the epidermis, a 1 × 1 cm skin sample was taken after tape stripping, and a 10-μm Tissue-Tek (Sakura Finetek, Tokyo, Japan)-embedded section was analyzed using a BZ-9000 Biorevo digital microscope (Keyence, Osaka, Japan) at the same time exposure.

An *in situ* dye permeability assay with toluidine blue was performed using embryos at 18 days (littermates). Unfixed, untreated embryos were dehydrated by a 1-minute incubation in an ascending series of methanol (25, 50, 74, and 100%) and rehydrated with the descending same methanol series, washed in PBS, and stained with 0.01% toluidine blue.

Scratching Behavior

Scratching behavior was measured in detail using the Sclaba Real system (Noveltec, Kobe, Japan). Mice were put into the machine 20 minutes before measurement to allow them to adapt to the new environment. Ointment was then applied, and the number and duration of scratching sessions were counted according to the manufacturer's protocol for 15 minutes.[20]

Dermatitis Models

For the assessment of irritant contact dermatitis, 20 μl of 0.2 mg/ml phorbol myristate acetate (PMA) (Sigma-Aldrich) was applied to both sides of the ears. Ear thickness change was measured at 1, 3, 12, and 24 hours as well as 5 days after application.

To induce a CHS response, 25 μl of 0.5% 1-fluoro-2.4-dinitrobenzene (DNFB) (Nacalai Tesque, Kyoto, Japan) was painted on the shaved abdomens of mice for sensitization. Five days later, the ears were challenged with 20 μl of 0.2% DNFB, and ear thickness change was measured at 24 and 48 hours after application. Nonsensitized mice were used as a control. A delayed-type hypersensitivity response model was established using OVA (Sigma-Aldrich). Mice were sensitized with 200 μl of 0.5 mg/ml of OVA in complete Freund's adjuvant (Difco Laboratories, Detroit, MI) intraperitoneally and challenged 5 days later with an injection of 20 μl of 1 mg/ml of OVA in incomplete Freund's adjuvant (Difco Laboratories) into the hind footpads. Footpad thickness was measured before and 24 hours after challenge. Nonsensitized mice were used as a control. Footpad swelling was calculated by (footpad thickness change of sensitized mice) − (footpad thickness change of nonsensitized mice). To induce murine AD-like skin lesions, 40 mg of 0.5% Dp in white petrolatum was topically applied to the ears and upper back twice a week for 8 weeks. Petrolatum without Dp was used as a control. One gram of Dp body product (Biostir) contained 1.78 mg of total protein with 2.47 μg of Dp protein (Der p1). Ear thickness and clinical scores were measured every week. Mite-specific IgE levels, TEWL, and histological appearance of eczematous skin were observed 12 hours after the final application.

Statistical Analysis

Data were analyzed using an unpaired two-tailed *t*-test. $P < 0.05$ was considered to be significant.

Results

Spontaneous Dermatitis of Flg^{ft} *Mice in the Steady State under SPF Conditions*

As described previously,[14,15] the expression of the filaggrin monomer was barely detectable by Western blotting in the dorsal skin of *Flg^{ft}* mice compared with that of B6 mice (data not shown). Here, we investigated the clinical manifestations seen in the skin of *Flg^{ft}* mice raised in a steady state under SPF conditions and found that *Flg^{ft}* mice developed spontaneous dermatitis (Figure 1A). The clinical severities of skin lesions, including pruritic activity, erythema, edema, erosion, and scaling, were scored. The total clinical scores of *Flg^{ft}* mice increased with age

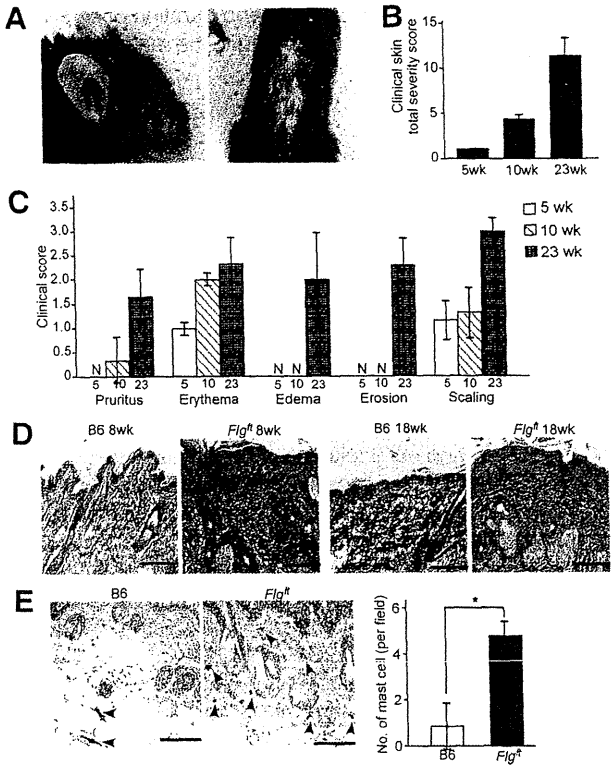

Figure 1. Spontaneous dermatitis in *Flg*^{ft} mice in SPF. **A:** Clinical photographs of 20-week-old *Flg*^{ft} mice. Total clinical severity scores (**B**) for each particular item (**C**) in 5-, 10- and 23-week-old *Flg*^{ft} mice. N, none. **D:** H&E-stained sections in 8- and 18-week-old mice. Scale bar = 100 μm. **E:** Toluidine blue staining of the skin from 8-week-old B6 and *Flg*^{ft} mice and the numbers of mast cells (**arrowheads**) per field are shown. $^*P < 0.05$.

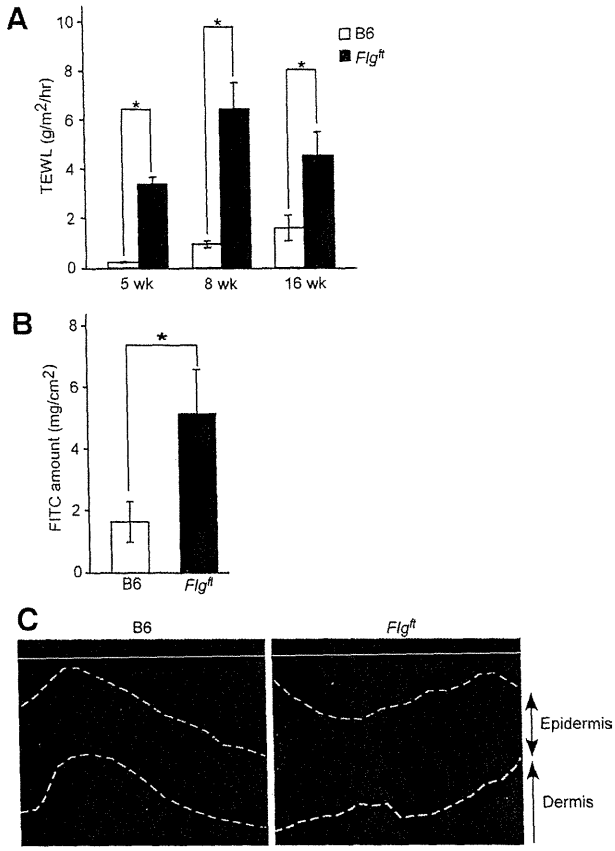

Figure 2. Skin barrier dysfunction in *Flg*^{ft} mice. **A:** TEWL through dorsal skin of 5-, 8-, and 16-week-old B6 and *Flg*^{ft} mice. **B:** Amount of FITC in the skin of B6 and *Flg*^{ft} mice after topical application. **C:** Fluorescence intensities of FITC of the skin after topical application. **Dashed white lines** indicate the border between the epidermis and the dermis, and the top of the epidermis. $^*P < 0.05$.

(Figure 1B). The first manifestations to appear when mice were young were erythema and fine scaling; pruritic activity, erosion, and edema followed later (Figure 1C). In contrast, no cutaneous manifestation was observed in either B6 mice, studied as a control, or heterozygous mice intercrossed with *Flg*^{ft} and B6 mice kept under SPF conditions throughout the experimental period (data not shown). In addition, there was no apparent difference in terms of clinical manifestations between the genders of *Flg*^{ft} mice throughout the period (data not shown).

Histological examination of skin from *Flg*^{ft} mice revealed epidermal acanthosis, increased lymphocyte infiltration, and dense fibrous bundles in the dermis in both younger (8-week-old) and older (18-week-old) *Flg*^{ft} mice; none of these were observed in B6 mice (Figure 1D). In addition, toluidine blue staining to detect mast cells showed an increased number of mast cells, especially degranulated mast cells in the upper dermis, in *Flg*^{ft} mice (Figure 1E). No mouse or human mite bodies were detected in the sections. These data support the diagnosis of spontaneous clinical dermatitis in *Flg*^{ft} mice in the steady state under SPF conditions.

Defect of Skin Barrier Function in Flg^{ft} *Mice*

Because barrier dysfunction is a common characteristic of AD,[4–7,21] we measured TEWL, an established indicator of barrier function.[21] TEWL was significantly higher in *Flg*^{ft} mice than in B6 mice from an early age (4 weeks) to an older age (16 weeks) (Figure 2A). Because TEWL is only a measure of water transportation through the skin from the inside to the outside of the body, another experimental method was necessary to evaluate outside-to-inside barrier function from the perspective of invasion of external stimuli. To address this issue, we measured FITC penetration through the skin from the outside. FITC solution was applied to the shaved dorsal skin of 8-week-old female mice; 3 hours later, the epidermis was separated and homogenized so that the FITC content could be measured with a fluorometer. The epidermis of *Flg*^{ft} mice contained a higher amount of FITC than that of B6 mice (Figure 2B). Neither group had FITC in the dermis after this procedure, however (data not shown). In addition, observation of fluorescence intensities in the epidermis of both mice showed stronger fluorescence in *Flg*^{ft} mice (Figure 2C). To further analyze the skin permeability, we examined the mouse embryos by toluidine blue solution and showed that the *Flg*^{ft} embryo was entirely dye-permeable compared with the control littermate (Supplemental Figure S1, see *http://ajp.amjpathol.org*). These data strongly indicate a defect in the skin barrier of *Flg*^{ft}

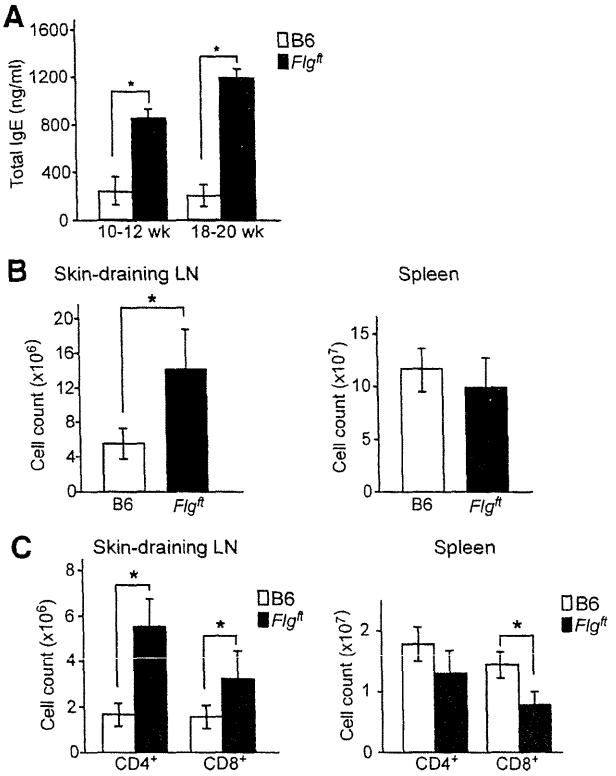

Figure 3. The immune status of *Flg*^{ft} mice in a steady state. **A:** Total serum IgE levels of B6 and *Flg*^{ft} mice as measured by enzyme-linked immunosorbent assay. **B** and **C:** Numbers of total cells (**B**), $CD4^+$ cells, and $CD8^+$ cells in the skin-draining LN and spleen (**C**). $^*P < 0.05$.

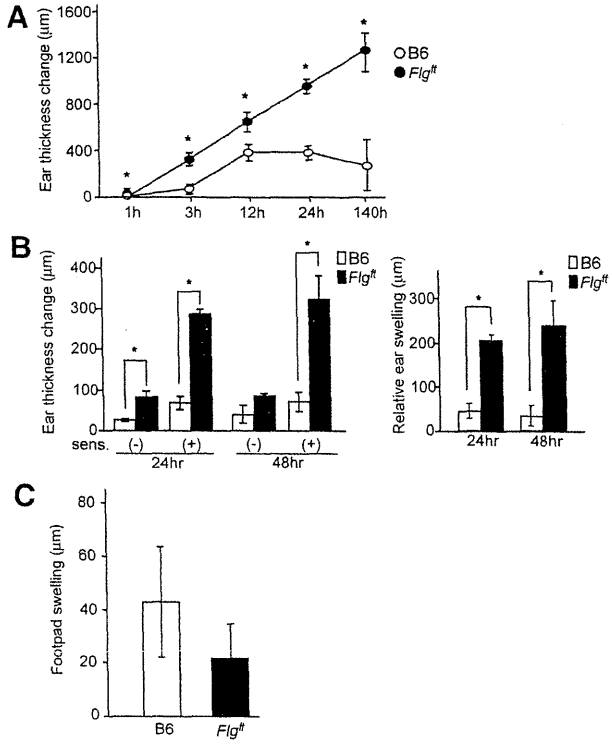

Figure 4. Enhanced cutaneous immune responses in *Flg*^{ft} mice. **A** and **B:** Ear thickness change in B6 and *Flg*^{ft} mice after topical application of PMA as a model of irritant contact dermatitis (**A**), after DNFB challenge on the ears with or without sensitization (**B, left panel**) and the relative ear swelling (**B, right panel**) as a model of CHS. **C:** Delayed-type hypersensitivity response. B6 and *Flg*^{ft} mice were intraperitoneally sensitized with OVA, and challenged through subcutaneous injection to the footpad. Twenty-four hours later, footpad swelling change was measured. $^*P < 0.05$.

mice, both from inside to outside and from outside to inside.

Immune Status in the Steady State

To further elucidate the immune status of *Flg*^{ft} mice in the steady state under SPF conditions, we measured the levels of total serum IgE, because increased severity of AD is known to be correlated with elevated serum IgE levels.[22] IgE levels were significantly higher in *Flg*^{ft} mice than in age-matched B6 mice in the steady state under SPF conditions (Figure 3A). To investigate this matter in greater detail, single cell suspensions from the skin-draining inguinal and axillary LNs and from the spleen were analyzed. The total mononuclear cell number of the LNs was significantly higher in *Flg*^{ft} mice than in B6 mice, but that of the spleen was comparable (Figure 3B). In addition, *Flg*^{ft} mice exhibited significantly higher numbers of $CD4^+$ and $CD8^+$ cells in the skin-draining LNs, but not in the spleen (Figure 3C). Thus, an enhanced immune reaction seems to be induced in *Flg*^{ft} mice by the condition of their skin.

To further analyze the immune condition of the skin, we measured the Th1 (interferon-γ [IFN-γ]), Th2 (interleukin [IL]-4 and IL-13), and Th17 (IL-17) cytokine mRNA levels of dorsal skin of 9-week-old mice in the steady state. The mRNA expression levels of IFN-γ, IL-4, and IL-13 were similar between *Flg*^{ft} and B6 mice, but there was an enhancement in the IL-17 mRNA expression (data not shown) as reported previously.[17]

Enhanced Dermatitis in Flg^{ft} *Mice under External Stimuli*

To characterize the likelihood of various cutaneous immune responses, mice were exposed to various external stimuli. First, we studied the irritant contact dermatitis response to PMA as an irritant agent. When we applied PMA to the ears of B6 and *Flg*^{ft} mice, *Flg*^{ft} mice exhibited an enhanced ear swelling response compared with age-matched B6 mice throughout the experimental period (Figure 4A). Next, we measured the CHS response to DNFB. DNFB was applied to the abdominal skin for sensitization; 5 days later, the ears were challenged with the same hapten. The ear thickness change was more prominent in *Flg*^{ft} mice than in B6 mice (Figure 4B, left panel). On the other hand, the ear thickness change of mice without sensitization was higher for *Flg*^{ft} mice than B6 mice, suggesting that irritation contact dermatitis was enhanced in *Flg*^{ft} mice as expected. To avoid the involvement of this irritation in CHS, we next analyzed the relative ear swelling by subtracting the ear thickness change without sensitization from the ear thickness change with sensitization. The relative ear swelling was more exten-

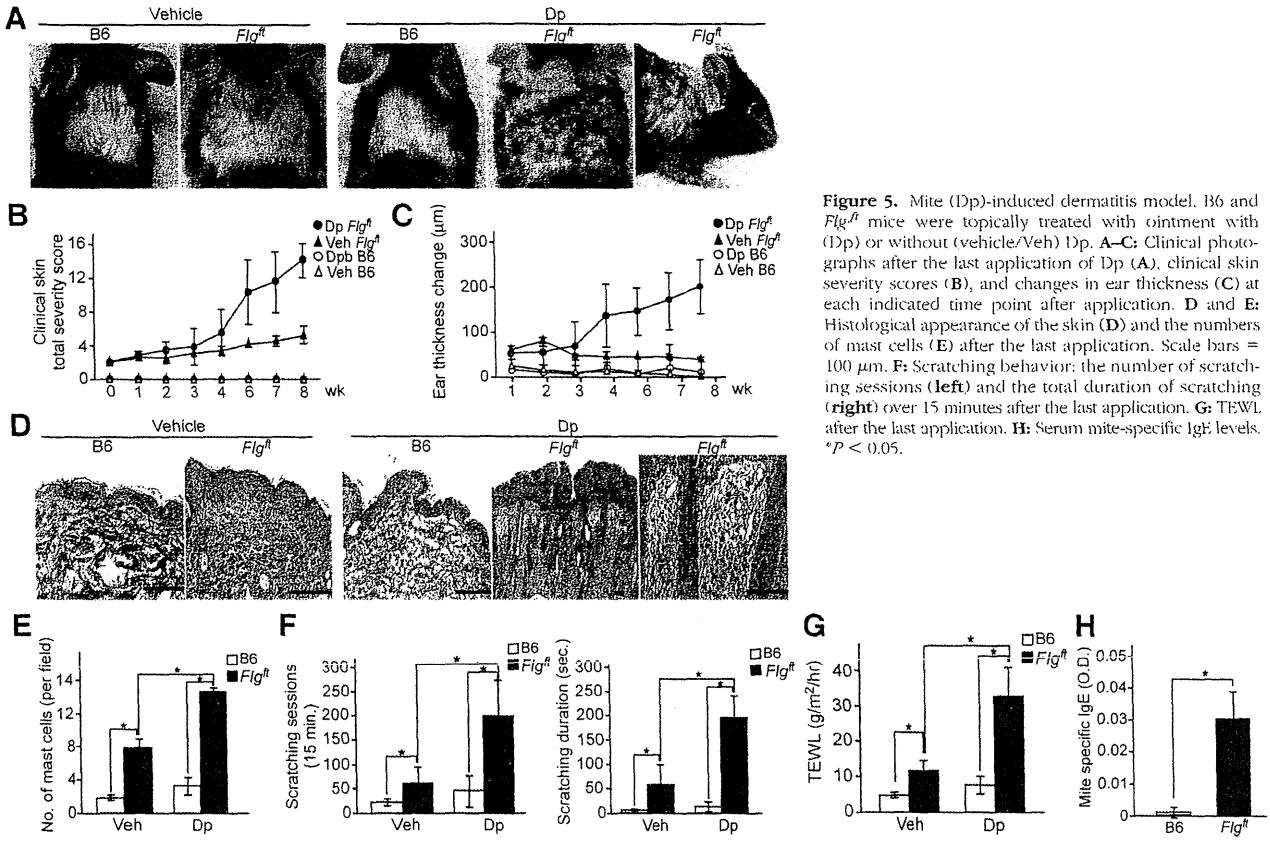

Figure 5. Mite (Dp)-induced dermatitis model. B6 and *Flg*^{ft} mice were topically treated with ointment with (Dp) or without (vehicle/Veh) Dp. **A–C:** Clinical photographs after the last application of Dp (**A**), clinical skin severity scores (**B**), and changes in ear thickness (**C**) at each indicated time point after application. **D** and **E:** Histological appearance of the skin (**D**) and the numbers of mast cells (**E**) after the last application. Scale bars = 100 μm. **F:** Scratching behavior: the number of scratching sessions (**left**) and the total duration of scratching (**right**) over 15 minutes after the last application. **G:** TEWL after the last application. **H:** Serum mite-specific IgE levels. $^{*}P < 0.05$.

sive in *Flg*^{ft} mice than in B6 mice (Figure 4B, right panel). We then measured the relative amount of mRNA for IFN-γ, as a representative Th1 cytokine, to GAPDH as an endogenous control. The relative amount of IFN-γ was higher in the ears of *Flg*^{ft} mice than in those of B6 mice 12 hours after the challenge (0.27 ± 0.13 versus 0.019 ± 0.013, $n = 3$). To further assess the immune responses of *Flg*^{ft} mice, we elicited a delayed-type hypersensitivity response through nonepicutaneous sensitization and challenge. Mice were immunized intraperitoneally with OVA and challenged with a subcutaneous injection of OVA into the footpad. In contrast to the CHS response induced via the skin, the resulting footpad swelling in *Flg*^{ft} mice was lower rather than higher than that in B6 mice (Figure 4C). We also examined the production of mRNA levels of the spleen 3 days after intraperitoneal OVA injection, and it showed a similar level of IFN-γ between *Flg*^{ft} mice and B6 mice (relative mRNA amount to GAPDH: 0.011 ± 0.005 versus 0.016 ± 0.006, $n = 5$). Thus, Th1/Tc1 immune responses were enhanced in *Flg*^{ft} mice only when the stimuli operated via the skin, suggesting that the enhanced immune responses seen in *Flg*^{ft} mice depend on skin barrier dysfunction.

It has been reported that *Flg*^{ft} mice show an enhanced immune response to OVA.[15,17] Their reaction to clinically relevant allergens such as mites has not been evaluated, however. It has also been reported that BALB/c or NC/Nga mice develop an allergic cutaneous immune response to mite antigens when they are applied to the skin after vigorous barrier disruption by means of tape-stripping or SDS treatment.[23,24] Accordingly, we sought to determine whether skin lesions could be induced in *Flg*^{ft} mice through the application of Dp ointment without any skin barrier disruption procedures to evaluate the physiological significance of filaggrin.

The application of Dp ointment to shaved backs and ears induced no cutaneous manifestation in B6 mice throughout the experimental period (Figure 5, A and B), but the same treatment induced dermatitis in *Flg*^{ft} mice, especially on the ears, face, and dorsal skin. Petrolatum alone, used instead of Dp ointment as a control, induced no skin manifestation (Figure 5, A–C). The clinical severity of Dp-induced dermatitis was scored; after 16 applications of Dp ointment over 8 weeks, *Flg*^{ft} mice had developed a very severe skin condition in contrast with the control groups. Consistently, ear swelling in response to Dp ointment was most prominent in *Flg*^{ft} mice (Figure 5C). Histological examination of H&E-stained sections of involved *Flg*^{ft} skin after 16 applications showed acanthosis, elongation of rete ridges, and dense lymphocyte and neutrophil infiltration in the dermis (Figure 5D), accompanied by an increased number of mast cells in the dermis (Figure 5E). We also measured the scratching behavior of *Flg*^{ft} mice treated with Dp using the Sclaba Real system. The number of scratching sessions and the total duration of scratching were significantly higher in *Flg*^{ft} mice than in B6 mice, even among those mice that had not been treated with Dp ointment (Figure 5F); treatment of *Flg*^{ft} mice with Dp ointment raised the number of scratching sessions and the total duration of scratching even higher.

We further evaluated barrier function by measuring TEWL in Dp-treated and untreated mice of each genotype; TEWL was higher in untreated *Flg*^{ft} mice than in B6 mice, and Dp treatment of *Flg*^{ft} mice raised TEWL even higher (Figure 5G). Finally, we examined mite-specific serum IgE levels after the last application and found that *Flg*^{ft} mice had higher levels of Dp-specific IgE than B6 mice had (Figure 5H). Thus, the treatment of *Flg*^{ft} mice with Dp ointment, even without prior barrier disruption, remarkably enhanced both the clinical manifestations and the laboratory findings that correspond to indicators of human AD.

Discussion

Here, we demonstrated that *Flg*^{ft} mice exhibit spontaneous dermatitis with lymphadenopathy, elevated IgE levels, and skin barrier disruption in a steady state under SPF conditions. These outcomes are compatible with the features of human AD, which include chronic eczema, pruritus, and dry skin with elevated TEWL and serum IgE levels.[1–4,25,26] In addition, *Flg*^{ft} mice exhibit enhanced susceptibility to irritant contact dermatitis, CHS, and mite-induced dermatitis compared with B6 mice; these characteristics are also reminiscent of human AD. These results suggest that the barrier defect in this strain of mice leads to spontaneous dermatitis and enhances cutaneous immune responses and inflammation.

Since the first introduction of *Flg*^{ft} mice in 1972,[13] there have been only a few reports of these mice. The first report demonstrated that *Flg*^{ft} mice without the *ma* mutation showed flaky skin as early as postnatal day 2 but became normal in appearance by 3 to 4 weeks of age without spontaneous dermatitis except for their slightly smaller ears.[13] Later, the lack of filaggrin in the epidermis was proposed in the commercially available strain of *Flg*^{ft} mice used in this study, which has both *Flg* and *ma* mutations, as a model of ichthyosis vulgaris, and therefore the cutaneous inflammatory conditions from the perspective of AD was not discussed.[14] There have been three recent studies using *Flg*^{ft} mice as a model of filaggrin deficiency: Fallon et al[15] used *Flg*^{ft} mice from which the *ma* mutation had been eliminated with four additional backcrosses to B6 mice, and others used the commercially available *Flg*^{ft} mice.[16,17] The first report showed only a histological abnormality without clinical manifestations,[15] the second report demonstrated spontaneous eczematous skin lesions after 28 weeks of age,[17] and the third report did not indicate any spontaneous dermatitis in *Flg*^{ft} mice.[16] In our experiment, we observed a spontaneous dermatitis as early as 5 weeks of age with mild erythema and fine scales. These symptoms gradually exacerbated, accompanied by scratching, erosion, and edema, respectively, and became prominent at the age of 23 weeks. The discrepancies among these results seem to be related to the presence or absence of the *ma* mutation and/or variation in the genetic backgrounds of the different strains used and to environmental factors. It has been reported that Japan has higher morbidity for AD than other countries,[27,28] possibly attributable to environmental factors such as pollen.

It has been reported that TEWL, an indicator of inside-to-outside barrier function, is high in both AD patients with the *FLG* mutation[29] and *Flg*^{ft} mice.[15] In consideration of the immunological defense by the skin, however, it is more important to assess outside-to-inside barrier function rather than inside-to-outside barrier function. In fact, outside-to-inside barrier dysfunction has recently been proposed as the most important aspect in the pathogenesis of AD.[9,26] Scharschmidt et al[16] reported increased bidirectional paracellular permeability of water-soluble xenobiotes by ultrastructural visualization in *Flg*^{ft} mice, suggesting a defect of the outside-to-inside barrier. However, the quantitative measurement of this parameter has not been addressed. Here, we propose a new method for evaluating outside-to-inside barrier function quantitatively by measuring the penetrance of FITC through the skin. This method has a parallel correlation with the qualitative measurement of FITC penetrated in epidermis and an established method for skin permeability assay, the *in situ* dye staining method. Therefore, by using this new method, we were able to detect outside-to-inside barrier dysfunction in *Flg*^{ft} mice quantitatively.

The skin abnormality associated with AD is well known to be a predisposing factor to sensitive skin[30,31] and allergic contact dermatitis,[32,33] but patients with AD produce a tuberculin response similar to that of healthy control subjects.[34,35] In humans, sensitive skin is defined as reduced tolerance to cutaneous stimulation, with symptoms ranging from visible signs of irritation to subjective neurosensory discomfort.[30,31] The question of whether human AD patients are more prone to allergic contact dermatitis than nonatopic individuals is still controversial.[33] To address this question, we evaluated skin responsiveness to PMA as an irritant and found that irritant contact dermatitis was enhanced in *Flg*^{ft} mice. In addition, *Flg*^{ft} mice showed an increased skin-sensitized CHS reaction, a form of classic Th1- and Tc1-mediated delayed-type hypersensitivity to haptens, emphasized by increased IFN-γ production. In contrast, when mice were sensitized intraperitoneally, no difference was observed between *Flg*^{ft} and B6 mice *in vivo* or *in vitro*. This finding is consistent with the observation that humans with and without AD respond comparably to tuberculin tests[34,35] and suggests that skin barrier function regulates cutaneous immune conditions, which hints at a possible mechanism involved in human AD.

Clinical studies have provided evidence that a house dust mite allergen plays a causative or exacerbating role in human AD[36] and that a strong correlation exists between patients with *FLG* null alleles and house dust mite-specific IgE.[37] AD-like skin lesions can be induced by repeated topical application of a mite allergen in NC/Nga mice but not in BALB/c mice.[23] In the present study, we induced skin lesions that were clinically and histologically similar to AD, along with increased TEWL, increased scratch behavior, and increased levels of mite-specific IgE, in *Flg*^{ft} mice through the application of Dp. Dp is a common aeroallergen that is frequently involved in induction of human AD. It has protease activities, spe-

cifically from Der p1, Der p3, and Der p9, which may activate protease-activated receptor-2 in human keratinocytes.[38,39] A recent report has shown that activation of protease-activated receptor-2 through Dp application significantly delays barrier recovery rate in barrier function-perturbed skin or compromised skin.[39] Therefore, Dp may play a dual role in the onset of AD, both as an allergen and proteolytic signal and as a perturbation factor of the barrier function, leading to the persistence of eczematous skin lesions in AD.[39,40]

To address the issue of variable genetic background, we observed immune responses in mice of other genotypes, such as BALB/c and C3H, as controls, but both of these lines exhibited much less severe CHS responses compared with those in *Flg*^{ft} mice (data not shown), suggesting that the enhanced immune responses seen in *Flg*^{ft} mice were not solely due to their genetic background. The effect of the *ma* mutation in relation to the *ft* mutation in commercially available *Flg*^{ft} mice in the development of AD-like skin lesions needs to be clarified in future studies. Furthermore, our study showed that heterozygous mice intercrossed with *Flg*^{ft} mice and B6 mice did not develop spontaneous dermatitis. In this way they are unlike human AD patients, most of whom are heterozygous for the *FLG* mutation. Not only human studies but also additional mouse studies are required to clarify these relationships.

In this study, we have shown that *Flg*^{ft} mice exhibit spontaneous dermatitis resembling human AD, enhanced irritation dermatitis and a contact hypersensitivity response, and mite-induced AD-like skin lesions, which provide hints for possible mechanisms in the human disease. These results suggest that *Flg*^{ft} mice have the potential to serve as an animal model of human AD and further accentuate the important role of filaggrin in skin barrier function in the pathogenesis of AD.

References

1. Jin H, He R, Oyoshi M, Geha RS: Animal models of atopic dermatitis. J Invest Dermatol 2009, 129:31–40
2. Wollenberg A, Bieber T: Atopic dermatitis: from the genes to skin lesions. Allergy 2000, 55:205–213
3. Novak N, Bieber T, Leung DY: Immune mechanism leading to atopic dermatitis. J Allergy Clin Immunol 2003, 112:S128–S139
4. Elias PM, Hatano Y, Williams ML: Basis for the barrier abnormality in atopic dermatitis: outside-inside-outside pathogenic mechanism. J Allergy Clin Immunol 2008, 121:1337–1343
5. Palmer CN, Irvine AD, Terron-Kwiatkowski A, Zhao Y, Liao H, Lee SP, Goudie DR, Sandilands A, Campbell LE, Smith FJ, O'Regan GM, Watson RM, Cecil JE, Bale SJ, Compton JG, DiGiovanna JJ, Fleckman P, Lewis-Jones S, Arseculeratne G, Sergeant A, Munro CS, El Houate B, McElreavey K, Halkjaer LB, Bisgaard H, Mukhopadhyay S, McLean WH: Common loss-of function variants of the epidermal barrier protein filaggrin are a major predisposing factor for atopic dermatitis. Nat Genet 2006, 38:441–446
6. Nomura T, Sandilands A, Akiyama M, Liao H, Evans AT, Sakai K, Ota M, Sugiura H, Yamamoto K, Sato H, Palmer CN, Smith FJ, McLean WH, Shimizu H: Unique mutations in the filaggrin gene in Japanese patients with ichthyosis vulgaris and atopic dermatitis. J Allergy Clin Immunol 2007, 119:434–440
7. Morar N, Cookson WO, Harper JI, Moffat MF: Filaggrin mutations in children with severe atopic dermatitis. J Invest Dermatol 2007, 127:1667–1672
8. Dale BA: Filaggrin, the matrix protein of keratin. Am J Dermatopathol 1985, 7:65–68
9. Listwan P, Rothnagel JA: Keratin bundling proteins. Methods Cell Biol 2004, 78:817–827
10. Candi E, Schmidt R, Melino G: The cornified envelope: a model of cell death in the skin. Nat Rev Mol Cell Biol 2005, 6:328–340
11. Gan SQ, McBride OW, Idler WW, Markova N, Steinert RM: Organization, structure, and polymorphisms of the human profilaggrin gene. Biochemistry 1990, 29:9432–9440
12. Shiohara T, Hayakawa J, Mizukawa Y: Animal models for atopic dermatitis: are they relevant to human disease? J Dermatol Sci 2004, 36:1–9
13. Lane P: Two new mutations in linkage group XVI of the house mouse. J Hered 1972, 63:135–140
14. Presland RB, Boggess D, Lewis SP, Hull C, Fleckman P, Sundberg JP: Loss of normal profilaggrin and filaggrin in flaky tail (ft/ft) mice: an animal model for the filaggrin-deficient skin disease ichthyosis vulgaris. J Invest Dermatol 2000, 115:1072–1081
15. Fallon PG, Sasaki T, Sandilands A, Campbell LE, Saunders SP, Mangan NE, Callanan JJ, Kawasaki H, Shiohama A, Kubo A, Sundberg JP, Presland RB, Fleckman P, Shimizu N, Kudoh J, Irvine AD, Amagai M, McLean WH: A homozygous frameshift mutation in the mouse Flg gene facilitates enhanced percutaneous allergen priming. Nat Genet 2009, 41:602–608
16. Scharschmidt TC, Man MQ, Hatano Y, Crumrine D, Gunathilake R, Sundberg JP, Silva KA, Mauro TM, Hupe M, Cho S, Wu Y, Celli A, Schmuth M, Feingold KR, Elias PM: Filaggrin deficiency confers a paracellular barrier abnormality that reduces inflammatory thresholds to irritants and haptens. J Allergy Clin Immunol 2009, 124:496–506, 506.e1–e6
17. Oyoshi MK, Murphy GF, Geha RS: Filaggrin-deficient mice exhibit Th17-dominated skin inflammation and permissiveness to epicutaneous sensitization with protein antigen. J Allergy Clin Immunol 2009, 124:475–493, 493.e1
18. Leung DY, Hirsch RL, Schneider L, Moody C, Takaoka R, Li SH, Meyerson LA, Mariam SG, Goldstein G, Hanifin JM: Thymopentin therapy reduces the clinical severity of atopic dermatitis. J Allergy Clin Immunol 1990, 85:927–933
19. Mori T, Kabashima K, Yoshiki R, Sugita K, Shiraishi N, Onoue A, Kuroda E, Kobayashi M, Yamashita U, Tokura Y: Cutaneous hypersensitivities to hapten are controlled by IFN-γ-upregulated keratinocyte Th1 chemokines and IFN-γ-downregulated Langerhans cell Th2 chemokines. J Invest Dermatol 2008, 128:1719–1727
20. Orito K, Chida Y, Fujisawa C, Arkwright PD, Matsuda H: A new analytical system for quantification scratching behavior in mice. Br J Dermatol 2004, 150:33–38
21. Gupta J, Grube E, Ericksen MB, Stevenson MD, Lucky AW, Sheth AP, Assa'ad AH, Khurana Hershey GK: Intrinsically defective skin barrier function in children with atopic dermatitis correlates with disease severity. J Allergy Clin Immunol 2008, 121:725–730
22. Novak N: New insights into the mechanism and management of allergic diseases: atopic dermatitis. Allergy 2009, 64:265–275
23. Kang JS, Lee K, Han SB, Ahn JM, Lee H, Han MH, Yoon YD, Yoon WK, Park SK, Kim HM: Induction of atopic eczema/dermatitis syndrome-like skin lesions by repeated topical application of a crude extract of Dermatophagoides pteronyssinus in NC/Nga mice. Int Immunopharmacol 2006, 6:1616–1622
24. Yamamoto M, Haruna T, Yasui K, Takahashi H, Iduhara M, Takaki S, Deguchi M, Arimura A: A novel atopic dermatitis model induced by topical application with Dermatophagoides farinae extract in NC/Nga mice. Allergol Int 2007, 56:139–148
25. Matsumoto M, Ra C, Kawamoto K, Sato H, Itakura A, Sawada J, Ushio H, Suto H, Mitsuishi K, Hikasa Y, Matsuda H: IgE hyperproduction through enhanced tyrosine phosphorylation of Janus kinase 3 in NC/Nga mice, a model for human atopic dermatitis. J Immunol 1999, 162:1056–1063
26. Cooper D, Hales J, Camp R: IgE-dependent activation of T cells by allergen in atopic dermatitis: pathophysiologic relevance. J Invest Dermatol 2004, 123:1086–1091
27. The International Study of Asthma and Allergies in Childhood (ISAAC) Steering Committee: Worldwide variation in prevalence of symptoms of asthma, allergic rhinoconjunctivitis, and atopic eczema: ISAAC. Lancet 1998, 351:1225–1232
28. Williams H, Robertson C, Stewart A, Aït-Khaled N, Anabwani G,

Anderson R, Asher I, Beasley R, Björkstèn B, Burr M, Clayton T, Crane J, Ellwood P, Keil U, Lai C, Mallol J, Martinez F, Mitchell E, Montefort S, Pearce N, Shah J, Sibbald B, Strachan D, von Mutius E, Weiland S: Worldwide variations in the prevalence of symptoms of atopic eczema in the international study of asthma and allergies in childhood. J Allergy Clin Immunol 1999, 103:125–138

29. Nemoto-Hasebe I, Akiyama M, Nomura T, Sandilands A, McLean WHI, Shimizu H: Clinical severity correlates with impaired barrier in filaggrin-related eczema. J Invest Dermatol 2009, 129:682–689
30. Willis CM, Shaw S, De Lacharrière O, Baverel M, Reiche L, Jourdain R, Bastien P, Wilkinson JD: Sensitive skin: an epidemiological study. Br J Dermatol 2001, 145:258–263
31. Farage MA, Katsarou A, Maibach HI: Sensory, clinical and physiological factors in sensitive skin: a review. Contact Dermatitis 2006, 55:1–14
32. Clayton TH, Wilkinson SM, Rawcliffe C, Pollock B, Clark SM: Allergic contact dermatitis in children: should pattern of dermatitis determine referral? A retrospective study of 500 children tested between 1995 and 2004 in one UK centre. Br J Dermatol 2006, 154:114–117
33. Mailhol C, Lauwers-Cances V, Rance F, Paul C, Giordano-Labadie F: Prevalence and risk factors for allergic contact dermatitis to topical treatment in atopic dermatitis: a study in 641 children. Allergy 2009, 64:801–806
34. Yilmaz M, Bingöl G, Altintas D, Kendirli SG: Correlation between atopic diseases and tuberculin responses. Allergy 2000, 55:664–667
35. Grüber C, Kulig M, Bergmann R, Guggenmoos-Holzmann I, Wahn U, MAS-90 Study Group: Delayed hypersensitivity to tuberculin, total immunoglobulin E, specific sensitization, and atopic manifestation in longitudinally followed early Bacille Calmette-Guérin-vaccinated and nonvaccinated children. Pediatrics 2001, 107:e36
36. Kimura M, Tsuruta S, Yoshida T: Correlation of house dust mite-specific lymphocyte proliferation with IL-5 production, eosinophilia, and the severity of symptoms in infants with atopic dermatitis. J Allergy Clin Immunol 1998, 101:85–89
37. Henderson J, Northstone K, Lee SP, Liao H, Zhao Y, Pembrey M, Mukhopadhyay S, Smith GD, Palmer CN, McLean WH, Irvine AD: The burden of disease associated with filaggrin mutations: a population-based, longitudinal birth cohort study. J Allergy Clin Immunol 2008, 121:872–877
38. Vasilopoulos Y, Cork MJ, Teare D, Marinou I, Ward SJ, Duff GW, Tazi-Ahnini R: A nonsynonymous substitution of cystatin A, a cysteine protease inhibitor of house dust mite protease, leads to decreased mRNA stability and shows a significant association with atopic dermatitis. Allergy 2007, 62:514–519
39. Jeong SK, Kim HJ, Youm JK, Ahn SK, Choi EH, Sohn MH, Kim KE, Hong JH, Shin DM, Lee SH: Mite and cockroach allergens activate protease-activated receptor 2 and delay epidermal permeability barrier recovery. J Invest Dermatol 2008, 128:1930–1939
40. Roelandt T, Heughebaert C, Hachem JP: Proteolytically active allergens cause barrier breakdown. J Invest Dermatol 2008, 128:1878–1880

The Journal of Immunology

Prostaglandin I2-IP Signaling Promotes Th1 Differentiation in a Mouse Model of Contact Hypersensitivity

Saeko Nakajima, Tetsuya Honda, Daiji Sakata, Gyohei Egawa, Hideaki Tanizaki, Atsushi Otsuka, Catharina Sagita Moniaga, Takeshi Watanabe, Yoshiki Miyachi, Shuh Narumiya and Kenji Kabashima

J. Immunol. published online Apr 16, 2010;
doi:10.4049/jimmunol.0903260

The Journal of Immunology is published twice each month by The American Association of Immunologists, Inc., 9650 Rockville Pike, Bethesda, MD 20814-3994.

Print ISSN: 0022-1767 Online ISSN: 1550-6606.

Published April 16, 2010, doi:10.4049/jimmunol.0903260

Prostaglandin I_2-IP Signaling Promotes Th1 Differentiation in a Mouse Model of Contact Hypersensitivity

Saeko Nakajima,* Tetsuya Honda,* Daiji Sakata,† Gyohei Egawa,*,‡ Hideaki Tanizaki,* Atsushi Otsuka,* Catharina Sagita Moniaga,* Takeshi Watanabe,‡ Yoshiki Miyachi,* Shuh Narumiya,† and Kenji Kabashima*,‡

PGI_2, which exerts its actions via its specific Gs-coupled I prostanoid receptor (IP), is known to be present in the lymph nodes, but its roles in acquired cutaneous immune responses remain unclear. To investigate the role of PGI_2-IP signaling in cutaneous immune responses, we applied IP-deficient ($Ptgir^{-/-}$) mice to contact hypersensitivity as a model of acquired immune response and found that $Ptgir^{-/-}$ mice exhibited a significantly decreased contact hypersensitivity response. Lymph node cells from sensitized $Ptgir^{-/-}$ mice exhibited decreased IFN-γ production and a smaller T-bet$^+$ subset compared with control mice. PGI synthase and IP expression were detected in dendritic cells and T cells, respectively, by quantitative real-time PCR analysis, suggesting that PGI_2 produced by dendritic cells acts on IP in T cells. In fact, in vitro Th1 differentiation was enhanced by an IP agonist, and this enhancement was nullified by protein kinase A inhibitor. These results suggest that PGI_2-IP signaling promotes Th1 differentiation through a cAMP-protein kinase A pathway and thereby initiates acquired cutaneous immune responses. *The Journal of Immunology*, **2010, 184: 000–000.**

The immune system defends the host against pathogens and other noxious Ags. Upon invasion, APCs, such as dendritic cells (DCs), ingest and process Ags, then migrate to draining lymph nodes (LNs), where they present the Ags to naive T cells. Engagement of the Ag complex by TCRs triggers clonal expansion and differentiation of T cells, which determines the outcome of immune responses (1, 2). CD4$^+$ Th cells are differentiated into three subsets: Th1, Th2, and Th17 cells. Th1 cells are characterized by the secretion of IFN-γ, Th2 cells by the secretion of IL-4, IL-5, and IL-13, and Th17 cells by the secretion of IL-17A and IL-22. Similarly, CD8$^+$ cytotoxic T cells (Tcs) undergo differentiation into two subsets: Tc1 and Tc2. Th1 and Tc1s are responsible for cell-mediated immune reactions, such as delayed-type hypersensitivity, which is critical for the eradication of intracellular pathogens. Th2 cells elicit allergic/humoral immune responses against extracellular pathogens by producing optimal Abs, particularly those of the IgE and IgG1 subtypes, whereas Th17 cells mediate host immune response against extracellular bacteria, fungi, and other microbes (3).

During Ag presentation, the direction of T cell differentiation is determined by the strength of TCR stimulation and by a variety of cytokines and other mediators produced by APCs (4–6). For example, it has been reported that strong TCR stimulation tends to promote Th1 differentiation but suppress Th2 differentiation (4). IL-12, IL-4, and TGF-β plus IL-6 are key determinants that direct T cell differentiation into Th1, Th2, and Th17 cells, respectively. Although these cytokine-directed pathways establish the basic framework for T cell differentiation, other noncytokine substances in the local milieu, such as prostanoids, may influence its balance (7, 8).

Prostanoids, which include PGD_2, PGE_2, $PGF_{2\alpha}$, PGI_2, and thromboxane A_2, are metabolites of arachidonic acid and are produced by sequential actions of cyclooxygenase (COX) and its respective synthases (8, 9). They are formed in response to various stimuli, and each regulates pathophysiological processes through its own receptor or receptors. For example, PGE_2 exerts its effect through four subtypes of receptors: EP1, EP2, EP3, and EP4. PGE_2 inhibits Th1 cytokine production and T cell proliferation through EP2 and EP4 (10–14), but promotes Th1 differentiation through EP1 (15) and Th1 differentiation and Th17 expansion through EP4 (16). Another prostanoid that may be involved in Th differentiation is PGI_2 (also known as prostacyclin), which has been detected in the LN (17) and locally in atopic dermatitis and asthma in mice and humans (18–21). PGI_2 acts through the I prostanoid receptor (IP), which is known to bind to Gs to mediate physiological functions through cAMP (9). In addition, expression studies have revealed that PGI_2 mediates not only increased in cAMP levels but also phosphoinositide responses (22). It has been reported that PGI_2 analogs suppress Th1 and Th2 cytokine production in vitro (23). PGI_2 analogs also suppress asthmatic responses through the inhibition of airway DC functions and recruitment of Th2 cells into airways in mice (24, 25) and through inhibiting bronchoconstriction in humans (26, 27). These reports suggest that PGI_2-IP signaling has an immunosuppressive effect in Th2-related diseases. In contrast, it has been demonstrated that PGI_2 analogs suppress Th1 cytokine production in vitro (23) and

*Department of Dermatology, †Department of Pharmacology, and ‡Center for Innovation in Immunoregulative Technology and Therapeutics, Kyoto University Graduate School of Medicine, Kyoto, Japan

Received for publication October 6, 2009. Accepted for publication March 11, 2010.

This work was supported in part by Grants-in-Aid for Scientific Research from the Ministries of Education, Culture, Sports, Science and Technology, and Health, Labor, and Welfare of Japan.

Address correspondence and reprint requests to Dr. Kenji Kabashima, Department of Dermatology and Center for Innovation in Immunoregulative Technology and Therapeutics, Kyoto University Graduate School of Medicine, Yoshida, Sakyo-ku, Kyoto 606-8501, Japan. E-mail address: kaba@kuhp.kyoto-u.ac.jp

The online version of this article contains supplemental material.

Abbreviations used in this paper: BMDC, bone marrow-derived dendritic cell; CHS, contact hypersensitivity; COX, cyclooxygenase; db, dibutyryl; DC, dendritic cell; DNBS, dinitrobenzene sulfonic acid; DNFB, dinitrofluorobenzene; IP, I prostanoid receptor; LN, lymph node; ND, not detected; PGIS, PGI synthase; PKA, protein kinase A; Tc, cytotoxic T cell.

that IP deficiency results in increased respiratory syncytial virus-induced inflammation-associated weight loss with increased levels of IFN-γ (28), suggesting that IP signaling suppresses Th1-type immune responses. However, collagen-induced arthritis driven by both Th1 and Th17 has been shown to be mediated through IP signaling. Therefore, the role of IP in Th1- and Tc1-mediated immune responses has been the source of some controversy.

Contact hypersensitivity (CHS), which presents clinically as allergic contact dermatitis, is a form of classic Th1- and Tc1-mediated delayed-type hypersensitivity to haptens such as dinitrofluorobenzene (DNFB) (29, 30). Although IP is known to be present in LNs, its role in acquired cutaneous immune responses remains unclear. In this study, we examined the role of IP in a DNFB-induced CHS model using IP-deficient (*Ptgir*$^{-/-}$) mice as well as an IP agonist. Previous findings on the immunosuppressive effect of PGI$_2$-IP signaling on Th1 differentiation in vitro and in vivo (23, 28) led us to expect an enhanced CHS response in *Ptgir*$^{-/-}$ mice. Intriguingly, contrary to this expectation, the CHS response was markedly reduced in *Ptgir*$^{-/-}$ mice. In addition, an IP agonist enhanced Th1 differentiation under Th1-skewing conditions in vitro, and this enhancement was nullified by a protein kinase A (PKA) inhibitor. Consistent with this, dibutyryl (db)-cAMP, a cAMP analog, was found to induce a similar enhancement of Th1 differentiation. These results suggest the possibility that IP on T cells facilitate Th1/Tc1 immune responses in vitro and in vivo through cAMP-PKA signaling.

Materials and Methods

Animals

B6 and BALB/c mice were purchased from Japan SLC (Shizuoka, Japan). *Ptgir*$^{-/-}$ mice generated in our facility (31) were backcrossed >10 times onto B6 mice. Eight- to 10-wk-old female mice bred in specific pathogen-free facilities at Kyoto University (Kyoto, Japan) were used for all experiments. All experimental procedures were approved by the institutional animal care and use committee of Kyoto University Graduate School of Medicine (Kyoto, Japan).

Reagents and Abs

We purchased DNFB from Nacalai Tesque (Kyoto, Japan), dinitrobenzene sulfonic acid (DNBS) from Alfa Aesar (Ward Hill, MA), and iloprost from Cayman Chemical (Ann Arbor, MI). FITC, PE, PE-Cy5, PE-Cy7, allophycocyanin–anti-CD4, anti-CD8, anti-B220, anti-CD11c, anti-CD86, anti-MHC class II, anti-CD62L, anti-CD44, anti-CD207, anti–IL-4, anti–IFN-γ, and anti-CD11c mAbs were purchased from eBioscience (San Diego, CA). FITC-conjugated anti–T-bet Ab was purchased from Santa Cruz Biotechnology (Santa Cruz, CA). The cAMP analog db-cAMP and forskolin, the PKA agonist N^6-Bnz-cAMP, and the PKA inhibitor H-89 were purchased from Sigma-Aldrich (St. Louis, MO).

CHS protocol, adoptive transfer, and histology

The shaved abdominal skin of 8-wk-old female mice was sensitized with 25 μl 0.5% (w/v) DNFB in acetone/olive oil (4:1). On day 5 after this sensitization, the ears were challenged with an application of 20 μl 0.3% DNFB. Ear thickness was measured for each mouse before and 24 and 48 h after elicitation at a predetermined site with a micrometer, and the difference was referred to as ear swelling change.

For adoptive transfer, LN cells were prepared from the inguinal and axillary LNs of one mouse that had been sensitized with DNFB 5 d previously and transferred i.v. into one naive B6 mouse. One hour later, the ears of the recipient animals were challenged with 20 μl 0.3% DNFB, and ear thickness was measured. For irritant contact dermatitis, either 20 μl 0.3% DNFB or 20 μl 0.2 μg/ml PMA (Sigma-Aldrich) was applied to the ears without prior sensitization.

For histological examination, tissues were fixed with 10% formalin in PBS and then embedded in paraffin. Sections with a thickness of 5 μm were prepared and subjected to staining with H&E. The histological findings were evaluated as reported previously (32). In brief, samples were scored for the severity and character of the inflammatory response using a subjective grading scale. Responses were graded as follows: 0, no response; 1, minimal response; 2, mild response; 3, moderate response; and 4, marked response. The slides were blinded, randomized, and reread to determine the histology score. All studies were read by the same pathologist using the same subjective grading scale. The total histology score was calculated as the sum of scores, including inflammation, neutrophils, mononuclear cells, edema, and epithelial hyperplasia.

Bone marrow-derived DC culture and FITC-induced cutaneous DC migration assay

For bone marrow-derived DC (BMDC) induction, 5 × 10^6 BM cells were cultured in 10 ml medium supplemented with 10 ng/ml recombinant murine GM-CSF (PeproTech, London, U.K.) for 5 d using 10-cm tissue culture dishes (33). After washing, 1 × 10^6 BMDCs were further incubated in 1 ml of the same medium in a 24-well plate with or without 1 μg/ml LPS (Sigma-Aldrich) for another 24 h.

For FITC-induced cutaneous DC migration assay, mice were painted with 200 μl 1% FITC (Sigma-Aldrich) in acetone/dibutyl phthalate (1:1), and samples of axillary and inguinal LNs were taken for flow cytometric analysis.

Lymphocyte proliferation assay

RPMI 1640 (Sigma-Aldrich) containing 10% heat-inactivated FCS (Invitrogen, Carlsbad, CA), 5 × 10^{-5} M 2-ME, 2 mM L-glutamine, 25 mM HEPES (Mediatech, Manassas, VA), 1 mM nonessential amino acids, 1 mM sodium pyruvate, 100 U/ml penicillin, and 100 μg/ml streptomycin was used as culture medium. For DNBS-dependent proliferation, single-cell suspensions were prepared from skin draining inguinal and axillary LNs of mice 5 d postsensitization with DNFB on the abdomen. One million LN cells were cultured with or without 100 μg/ml DNBS sodium for 72 h, pulsed with 0.5 μCi [^{3}H]thymidine for the last 24 h, and subjected to liquid scintillation counting. For measurement of cytokine production, culture supernatants were collected 72 h postincubation.

ELISA and beads array

The amounts of IL-17, 6-keto PGF$_{1\alpha}$, and cAMP in the culture medium were measured by ELISA (IL-17, R&D Systems, Minneapolis, MN; 6-keto PGF$_{1\alpha}$, Cayman Chemical; cAMP, R&D Systems). The amounts of IFN-γ and IL-4 were measured using a cytometric bead array system (BD Biosciences, Franklin Lakes, NJ) according to the manufacturer's instructions. For the measurement of 6-keto PGF$_{1\alpha}$, CD11c$^+$ DCs and Thy1.2$^+$ T cells were sorted from the spleen using an auto MACS separator (Miltenyi Biotec, Bergisch Gladbach, Germany). A total of 3 × 10^5 DCs and T cells were incubated with or without LPS (100 ng/ml) and plate-bound anti-CD3 Ab (3 μg/ml) for 24 h, and the supernatants were collected for ELISA assays. For the measurement of cAMP, 3 × 10^5 T cells were pretreated with anti-CD3 and -CD28 Abs at indicated concentrations under Th1-skewing conditions, and stimulated with 0.5 mM 3-isobutyl-1-methylanthine (IBMX, Wako, Osaka, Japan) for 10 min. The cells were further incubated with or without the IP agonist (1 μM) for 10 min, and cAMP levels in the culture supernatant were measured by ELISA.

Th1 and Th2 differentiation assays and intracellular staining

B6 and BALB/c mice were used for Th1 and Th17 differentiation and Th2 differentiation assays, respectively. For naive CD4$^+$ CD62L$^+$ or CD8$^+$ CD62L$^+$ T cell purification, cells were sorted with the auto MACS separator (Miltenyi Biotec). The purity was confirmed to be >95% through flow cytometry using the FACSCanto II system (BD Biosciences). For in vitro Th1 and Tc1 differentiation assays, B6 CD4$^+$ T cells or CD8$^+$ T cells were stimulated for 2 d with plate-bound anti-CD3 (1 and 10 μg/ml) and anti-CD28 (0, 1, 10, and 100 μg/ml) Abs in combination with 10 ng/ml IL-12, 10 μg/ml anti–IL-4 Ab, and 20 ng/ml IL-2 (34) as the primary stimulation. Similarly, BALB/c naive CD4$^+$ T cells were incubated in the presence of 10 ng/ml IL-4, 10 μg/ml anti–IFN-γ Ab, and 20 ng/ml IL-2 for Th2 differentiation. Forty-eight hours after the primary stimulation for Th1 and Th2, cells were washed and cultured further under the Th1- and Th2-skewing conditions without anti-CD3 or anti-CD28 Ab stimulation.

For intracellular cytokine staining, cells were stimulated for 6 h with 50 ng/ml PMA and 1 μM ionomycin in the presence of GolgiStop (BD Biosciences). After washing, cells were fixed and permeabilized with Cytofix/Cytoperm buffer (BD Biosciences) according to the manufacturer's instructions (35).

For T-bet staining, cells were fixed and permeabilized with Cytofix/Cytoperm solution (BD Biosciences) and stained with FITC-conjugated anti–T-bet Ab.

MLR

CD4$^+$ T cell (1 × 10^6/well) and CD11c$^+$ DCs (1 × 10^4/well) purified with auto MACS (purity, >95% and 70%, respectively) were incubated together for 72 h, pulsed with 0.5 μCi [^{3}H]thymidine for the last 24 h, and subjected

to liquid scintillation counting. For measurement of cytokine production, culture supernatants were collected 72 h postincubation.

Quantitative PCR analysis

Cells were sorted with an FACSAria II cell sorter (BD Biosciences), and total RNAs were isolated with RNeasy kits and digested with DNase I (Qiagen, Hilden, Germany). cDNA was reverse transcribed from total RNA samples using the Prime Script RT reagent kit (Takara Bio, Otsu, Japan). Quantitative RT-PCR was performed by monitoring the synthesis of dsDNA during the various PCR cycles using SYBR Green I (Takara Bio) and the Light Cycler real-time PCR apparatus (Roche, Basel, Switzerland) according to the manufacturer's instructions. Primers for *Ptgir*, *Ptgis*, *Ptgs1*, and *Ptgs2* were obtained from Hokkaido System Science (Sapporo, Japan). The primer sequences were *Ptgir*, 5′-TGG GAC GAT GCT GTG TGA C-3′ (forward) and 5′-GAA AGC GTA GAT GGA AGG CAA-3′ (reverse); *Ptgis*, 5′-CAA ACA TGG AGG AAT CGT CTT CG-3′ (forward), 5′-GGG GGA CCA GAT TAA ATA GTG TG-3′ (reverse); *Ptgs1*, 5′-TCA ACG TGT TCC TCA AGT CGC-3′ (forward), 5′-AGG GTA TGG TTA CCG TCT CCC-3′ (reverse); and *Ptgs2*, 5′-ATG AGT ACC GCA AAC GCT TCT-3′ (forward), 5′-ACT GTA GAG GGC TTT CAA TTC TG-3′ (reverse). The cycling conditions were as follows: initial enzyme activation at 95°C for 10 min, followed by 40 cycles at 95°C for 10 s, and 60°C for 20 s. All cycling reactions were performed in the presence of 3.5 mM $MgCl_2$. Gene-specific fluorescence was measured at 60°C. For each sample, triplicate test reactions and a control reaction lacking reverse transcriptase were analyzed for expression of the genes, and results were normalized to those of the housekeeping GAPDH mRNA.

Western blotting

T cells (5×10^6 cells) and BMDCs (2×10^6 cells) were lysed and homogenated in cell lysis buffer (Cell Signaling Technology, Boston, MA). The supernatant (10,000 g, 10 min, 4°C) was used for immunoblotting with primary Abs against COX-2 (1:1000, Cayman Chemical), IP (1:500, Cayman Chemical), and PGI synthase (PGIS; 1:250, Cayman Chemical). HRP-conjugated secondary anti-rabbit IgG Ab (Cell Signaling Technology) was used for detection by ECL (Amersham Pharmacia, Piscataway, NJ).

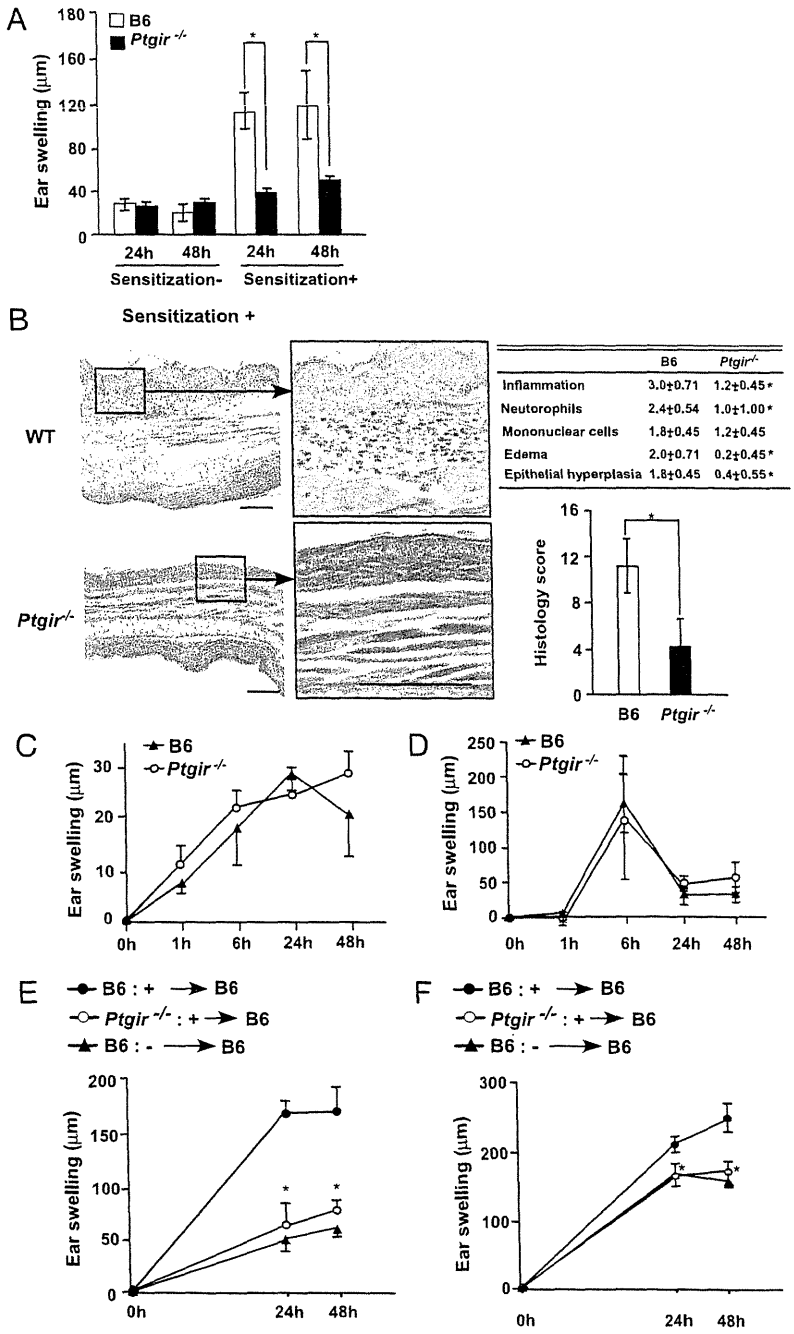

FIGURE 1. Impaired cutaneous immune response in $Ptgir^{-/-}$ mice. *A*, Impaired CHS response in $Ptgir^{-/-}$ mice. B6 and $Ptgir^{-/-}$ mice (n = 5 per group) were sensitized with DNFB or vehicle, and the ear swelling change was measured at 24 and 48 h postchallenge. *B*, H&E staining of the ears of sensitized B6 and $Ptgir^{-/-}$ mice 48 h postchallenge with DNFB (H&E, original magnification ×40 [*left panels*]; ×400 [*right panels*]). Scale bar, 100 μm (*left panels*). The histological findings were scored by inflammation, neutrophil infiltration, mononuclear cell infiltration, edema and epithelial hyperplasia (*right upper panel*). The total histology score is the sum of all scores. Data are presented as means ± SD (n = 5). *C* and *D*, Irritant contact dermatitis. DNFB (*C*) or PMA (*D*) was topically administered to the ears of B6 and $Ptgir^{-/-}$ mice (n = 5 per group), and ear swelling change was measured 1, 6, 24, and 48 h later. *E* and *F*, Inhibited CHS response in B6 mice after adoptive transfer of $Ptgir^{-/-}$ LN cells. LN cells (*E*) and further sorted Thy1.2$^+$ T cells from the LN cells (*F*) were prepared from DNFB-sensitized B6 or $Ptgir^{-/-}$ donors and adoptively transferred into naive B6 recipients. The recipients were challenged with 0.3% (*E*) and 0.5% (*F*) DNFB, and ear swelling was measured 24 and 48 h later (n = 5 per group). Data are presented as means ± SD, and each data point is representative of at least three experiments with similar results. *$p < 0.05$ versus corresponding B6 mice.

Statistical analysis

Unless otherwise indicated, data are presented as means ± SD. The p values were calculated with the two-tailed Student t test.

Results

Inhibition of CHS response in Ptgir$^{-/-}$ mice

To investigate the role of PGI$_2$-IP signaling in Th1- and Tc1-mediated immune responses, we used a DNFB-induced CHS model in control C57BL/6 (B6) and *Ptgir*$^{-/-}$ mice (35, 36). The severity of ear swelling in *Ptgir*$^{-/-}$ mice was much lower than that in B6 mice both 24 and 48 h postchallenge (Fig. 1*A*). Histology of the ears 48 h postchallenge showed considerable lymphocyte infiltration and edema in the dermis of sensitized B6 mice, which was less apparent in sensitized *Ptgir*$^{-/-}$ mice (Fig. 1*B*, *left panel*). The histology score in *Ptgir*$^{-/-}$ mice was lower than that in B6 mice (Fig. 1*B*, *right panel*). In addition, irritant contact dermatitis was induced for reference purposes through an application of DNFB or PMA to the ears of B6 and *Ptgir*$^{-/-}$ mice that had not been sensitized; we found comparable changes in ear thickness between these two groups at 1, 6, 24, and 48 h postchallenge (Fig. 1*C*, 1*D*). These results suggest that IP signaling enhanced the DNFB-induced CHS response, but did not enhance irritant contact dermatitis.

Next, we induced a CHS response through adoptive transfer to clarify the action phase of IP signaling. The recipients of LN cells or T cells purified from the LN cells of sensitized B6 mice showed an enhanced CHS response, whereas the recipients of the LN cells or T cells from sensitized *Ptgir*$^{-/-}$ mice showed a markedly inhibited response (Fig. 1*E*, 1*F*). These data indicate that IP signaling is, at least to some extent, mediated by T cells during the sensitization phase of the CHS response.

To further characterize the effect of IP during the sensitization phase of CHS, we analyzed and compared the compositions of LN cells in animals that had undergone sensitization of the skin and those that had not. Five days postsensitization, total cell numbers of LN cells and cell counts and frequencies of CD4$^+$ and CD8$^+$ T cell subsets were comparable between B6 and *Ptgir*$^{-/-}$ mice (Fig. 2*A*). In contrast, fewer CD44$^+$ CD62L$^-$ effector memory T cells were observed in *Ptgir*$^{-/-}$ mice than in B6 mice 5 d postsensitization, although the numbers of CD44$^-$ naive T cells and CD44$^+$ CD62L$^+$ central memory T cells among CD4$^+$ and CD8$^+$ T cell subsets were comparable (Fig. 2*B–D*). These results suggest that differentiation of naive T cells into effector memory T cells during the sensitization period might be inhibited in *Ptgir*$^{-/-}$ mice. Unsensitized *Ptgir*$^{-/-}$ mice showed no apparent abnormalities in the numbers of CD44$^-$ naive T cells, CD44$^+$ CD62L$^+$ central memory T cells, or CD44$^+$ CD62L$^-$ effector memory T cells compared with B6 mice (Fig. 2*B–D*).

Impaired IFN-γ production in draining LNs of Ptgir$^{-/-}$ mice after DNFB application

To evaluate the effect of IP signaling on T cell activation and differentiation, skin-draining LN cells were collected from B6 and *Ptgir*$^{-/-}$ mice that had been sensitized with DNFB 5 d prior. LN cell proliferation was then induced by restimulation with DNBS in vitro. The amount of proliferation observed was lower in *Ptgir*$^{-/-}$ mice than in B6 mice (Fig. 3*A*). In addition, the levels of IFN-γ induced by the DNBS challenge in vitro were markedly lower in cells from *Ptgir*$^{-/-}$ mice than in those from B6 mice (Fig. 3*B*), although the two groups exhibited comparable levels of IL-17 production (Fig. 3*B*). In addition, evidence of IL-4 production was not detected in the culture supernatant (Fig. 3*B*). We then analyzed the number of cells expressing T-bet, a key transcription factor in Th1 differentiation (27), in the draining LNs of B6 and *Ptgir*$^{-/-}$ mice 5 d postsensitization. The number of T-bet–expressing CD4$^+$ and CD8$^+$ T cells in *Ptgir*$^{-/-}$ mice was

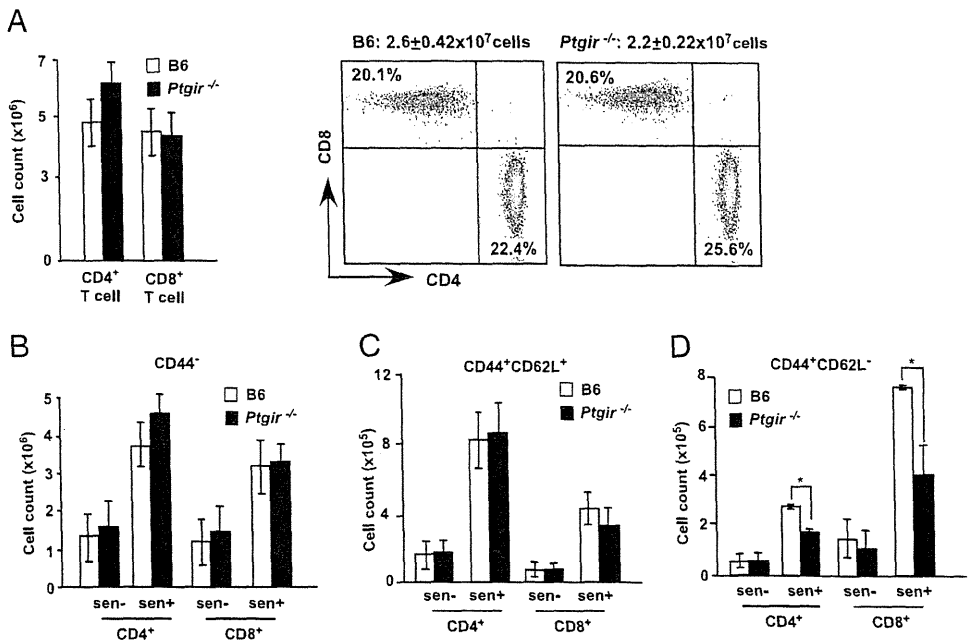

FIGURE 2. Impaired development of effector memory T cell subset in *Ptgir*$^{-/-}$ mice postsensitization. *A–D*, T cell subsets. Skin-draining inguinal and axillary LN cells were collected before and 5 d after DNFB application to the abdomens of B6 and *Ptgir*$^{-/-}$ mice (n = 5 per group), and the numbers of CD4$^+$ and CD8$^+$ T cells (*A*, *left panel*), CD44$^-$ naive (*B*), CD44$^+$ CD62L$^+$ central memory (*C*), and CD44$^+$ CD62L$^-$ effector memory (*D*) subsets of CD4$^+$ and CD8$^+$ T cells are shown. A representative flow cytometric plot of LN cells 5 d postsensitization is shown (*A*, *right panel*). The numbers located above the flow cytometric plots (*A*, *right panel*) are total numbers of LN cells. Data are presented as the means ± SEM and are representative of three independent experiments with similar results. $*p < 0.05$.

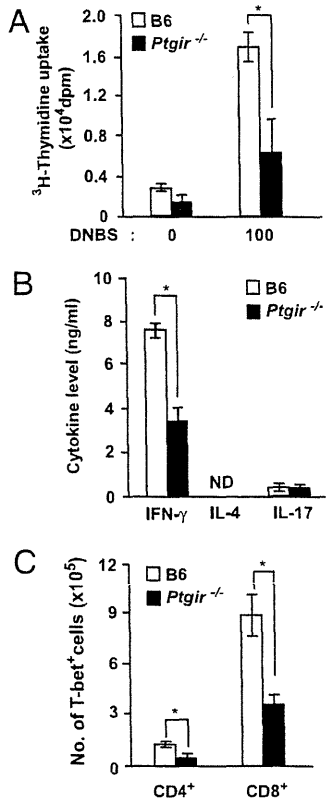

FIGURE 3. Decreased Th1 cytokine production in the LN of sensitized *Ptgir*$^{-/-}$ mice. *A* and *B*, DNBS-induced lymphocyte proliferation and cytokine production. Cells were collected from the LNs of B6 or *Ptgir*$^{-/-}$ mice 5 d after DNFB application and cultured for 3 d with or without 100 μg/ml DNBS. Cell proliferation was measured by [^{3}H]thymidine incorporation (n = 5 mice per group) (*A*). The amount of IFN-γ, IL-4, and IL-17 in the culture medium was measured by CBA (IFN-γ and IL-4) and ELISA (IL-17) (n = 5 mice per group). *C*, Numbers of T-bet$^+$ cells. The numbers of T-bet$^+$ CD4$^+$ and CD8$^+$ T cells from inguinal and axillary LNs were counted 5 d postsensitization with DNFB on the abdomen (n = 5 mice per group). Data are presented as the mean ± SD, and each data point is representative of three experiments with similar results. *$p < 0.05$ versus corresponding B6 mice. ND, not detected.

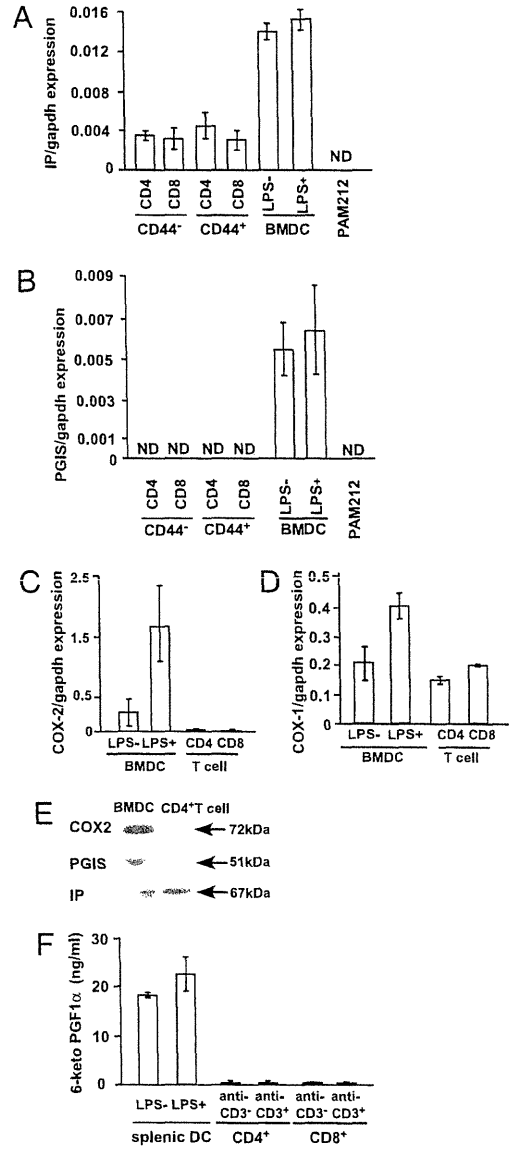

FIGURE 4. IP and PGI_2 expression on T cells and DCs. *A* and *B*, IP and PGIS expression. The *Ptgir* (IP) (*A*) and *Ptgis* (PGIS) (*B*) mRNA expressions in CD44$^-$ naive and CD44$^+$ memory CD4$^+$ and CD8$^+$ T cells of axillary and inguinal LNs, BMDCs stimulated with or without LPS and cells of the keratinocyte cell line PAM212 were evaluated through quantitative real-time PCR analysis, and arbitrary expression units are shown. *C* and *D*, COX-1 and COX-2 expression. The mRNA levels of *Ptgs1* (COX-1) and *Ptgs2* (COX-2) in BMDCs cultured in the presence or absence of LPS for 24 h and CD4$^+$ and CD8$^+$ T cells were measured, and arbitrary expression units are shown. *E*, Western blotting. IP, PGIS, and COX-2 protein levels were evaluated in BMDCs and T cells by Western blotting. *F*, PGI_2 production. Purified CD11c$^+$ DCs and Thy1.2$^+$ T cells from the spleen were incubated. 6-keto $PGF_{1\alpha}$, a stable metabolite of PGI_2, was abundant in the culture supernatant of DCs, but much less in the CD4$^+$ and CD8$^+$ T cell subsets. Data are presented as the mean ± SD (n > 3 per group), and each data point is representative of three independent experiments with similar results (*A–F*). ND, not detected.

significantly lower than that in B6 mice (Fig. 3*C*). These results indicate that the differentiation of naive T cells to Th1 cells/Tc1 is impaired in *Ptgir*$^{-/-}$ mice.

PGI_2 production by BMDCs and IP expression in DCs and T cells

The impaired production of Th1 cells that we observed in the draining LNs of *Ptgir*$^{-/-}$ mice indicated that IP signaling promoted Th1 differentiation through either DCs or naive T cells. To identify candidates for the action phase of PGI_2 in the initiation of CHS responses, we purified CD44$^-$ naive CD4$^+$ and CD8$^+$ T cells, CD44$^+$ memory CD4$^+$ and CD8$^+$ T cells, cells from the keratinocyte cell line PAM212, and BMDCs. IP expression was detected not only in BMDCs as expected, but also in both naive and memory T cells by quantitative PCR analysis (Fig. 4*A*). *Ptgir* mRNA, on the other hand, was not detected in the keratinocyte cell line PAM212 (Fig. 4*A*).

Next we sought to identify the type of cell that produces PGI_2. PGI_2 is produced through the sequential catalysis of COX and PGIS. COX enzymes have two molecular isoforms, constitutive COX-1 and inducible COX-2. mRNA of *Ptgis* (PGIS) was detected in BMDCs, and the level of this mRNA was minimally enhanced by LPS stimulation (Fig. 4*B*). In contrast, PGIS mRNA was not detected in CD4$^+$ T cells, CD8$^+$ T cells, or PAM212 (Fig. 4*B*). Our measurement of the expression levels of *Ptgs1* (COX-1) and *Ptgs2* (COX-2) mRNA revealed that whereas COX-1 was expressed in both BMDCs and T cells, mRNA levels of COX-2 were abundant in BMDCs (Fig. 4*C*, 4*D*). In addition, we evaluated

the expression levels of IP, PGIS, and COX-2 proteins in DCs and T cells by Western blotting. Consistent with the mRNA expressions, IP proteins were observed in both DCs and T cells, and PGIS and COX-2 proteins were detected mainly in DCs by Western blotting analysis (Fig. 4*E*). Because PGIS is essential for the production of PGI_2, the above results suggest that DCs are the major source of PGI_2 during the sensitization phase of the CHS response. In fact, 6-keto $PGF_{1\alpha}$, a stable metabolite of PGI_2, was abundant in the culture supernatant of DCs, but much less in the $CD4^+$ and $CD8^+$ T cell subsets (Fig. 4*F*). These results suggest that PGI_2 is produced by DCs and acts on IP located either on the DCs themselves or on T cells in the draining LNs to induce Th1/Tc1 immune responses.

Marginally enhanced DC functions due to IP deficiency

After encountering DNFB, cutaneous DCs, including Langerhans cells and dermal DCs, migrate to LNs with increased expression of MHC class II and costimulatory molecules and increased production of cytokines, one of which is IL-12, a key cytokine for Th1/Tc1 differentiation (1, 6, 37). It has been reported that IP on DCs in the lungs inhibited the functioning of DCs in a murine asthma model (24), but the roles of IP in cutaneous DCs in the CHS response remain unknown. Therefore, we compared the abundance, migration, and maturation of cutaneous DCs between B6 and $Ptgir^{-/-}$ mice during a CHS response. We painted FITC on the shaved abdominal skin of B6 and $Ptgir^{-/-}$ mice to evaluate the migration activity of cutaneous DCs. A marginal increase in the number of $FITC^+$ $CD11c^+$ MHC class II^+ cutaneous DCs migrating from the skin into the regional LNs was observed in $Ptgir^{-/-}$ mice 24 and 72 h after FITC application, but this increase was not statistically significant (Supplemental Fig. 1*A*). In addition, the number of $CD86^{high}$ DC subsets among $FITC^+$ $CD11c^+$ MHC class II^+ cutaneous DCs was elevated in $Ptgir^{-/-}$ mice, but, again, this difference from the B6 mice was not significant (Supplemental Fig. 1*B*). Similar findings were observed in $FITC^+$ $Langerin^+$ $CD11c^+$ MHC class II^+ Langerhans cells (Supplemental Fig. 1*C*) and $FITC^+$ $Langerin^-$ $CD11c^+$ MHC class II^+ dermal DCs (Supplemental Fig. 1*D*). In addition, we evaluated the T cell stimulatory capacity of $Ptgir^{-/-}$ DCs. BALB/c T cells were incubated with allogeneic B6 or $Ptgir^{-/-}$ splenic $CD11c^+$ DCs. Proliferation of T cells was not inhibited but rather tended to be enhanced by the deficiency of IP in DCs (Supplemental Fig. 1*E*). Similar findings were observed when we measured IFN-γ levels in the supernatants of this culture assay (data not shown). Therefore, the attenuation of the Th1/Tc1-mediated CHS response in $Ptgir^{-/-}$ mice cannot be explained by the regulation of DC functions through IP stimulation; instead, the mechanism must operate on some other cellular targets.

IP activation facilitates Th1 differentiation, but suppresses Th2 differentiation in vitro

To examine the direct action of IP in Th1 differentiation, we incubated $CD4^+$ T cells under Th1-skewing conditions (34) in the presence or absence of iloprost, an IP agonist, and assessed the extent of Th1 differentiation using flow cytometry. Under the Th1-skewing condition, the IP agonist marginally decreased the number of IFN-γ–producing cells in $CD4^+$ T cells isolated from B6 mice when CD28 engagement was absent (Fig. 5*A*). In contrast, when CD28 engagement was present,

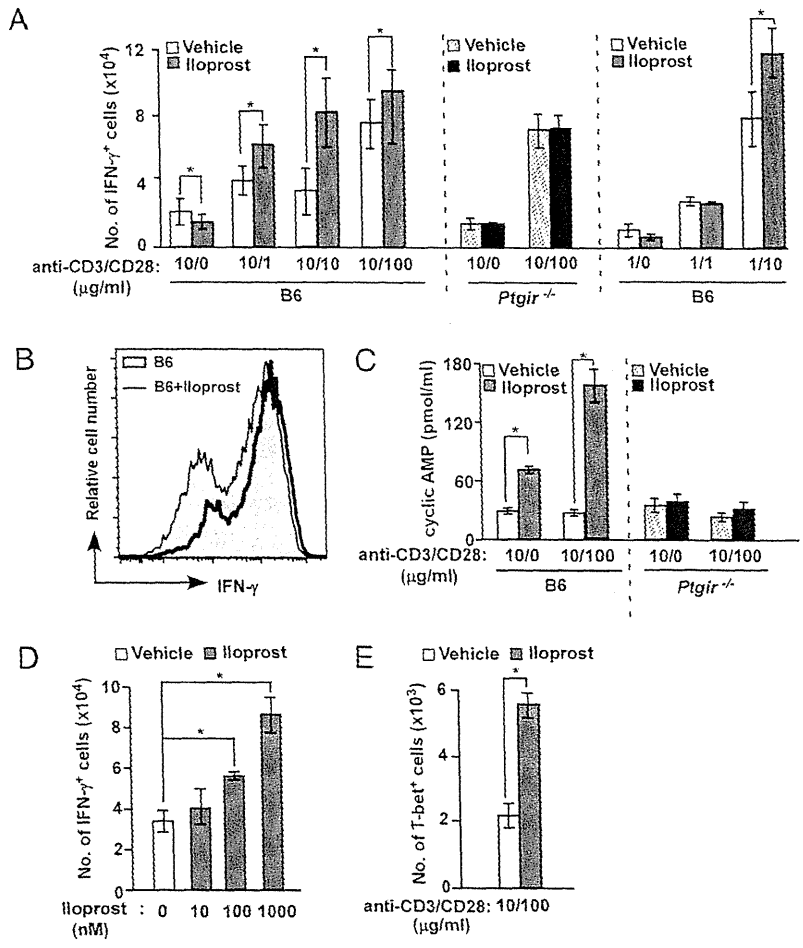

FIGURE 5. Effect of IP stimulation on T cell differentiation into Th1 subsets in vitro. *A–E*, Enhancement of Th1 differentiation by IP stimulation under strong anti-CD28 stimulation. $CD4^+$ T cells from B6 mice were cultured under Th1-skewing conditions with or without 1 μg/ml iloprost with plate-bound anti-CD3 and CD28 Abs at the indicated concentrations (μg/ml). The numbers of IFN-γ^+ cells per well in triple wells are shown (*A*). Representative flow cytometric histograms in the presence or absence of iloprost are shown (*B*). *C*, cAMP levels. T cells were pretreated with anti-CD3 and CD28 Abs at the indicated concentrations under Th1-skewing conditions for 3 d, incubated with iloprost for 10 min to evaluate the cAMP levels in the culture supernatant. *D*, Enhancement of Th1 differentiation by IP stimulation in a dose-dependent manner. $CD4^+$ T cells from B6 mice were cultured under Th1-skewing conditions with the indicated concentrations of iloprost in the presence of 10 μg/ml plate-bound anti-CD3 and 100 μg/ml plate-bound CD28 Abs. The numbers of IFN-γ^+ cells per well are shown. *E*, Increase of T-bet$^+$ cells by IP stimulation. The numbers of T-bet$^+$ cells are shown. Columns show the mean ± SD, and data are representative of three independent experiments with similar results. $*p < 0.05$.

the IP agonist significantly increased the number of IFN-γ–producing cells in a dose of anti-CD28 Ab-dependent manner (Fig. 5*A*, 5*B*). The enhancement of Th1 differentiation by the IP agonist was not detected when naive CD4$^+$ T cells from *Ptgir*$^{-/-}$ mice were used (Fig. 5*A*). Consistent with this, cAMP levels in the culture supernatant were increased by the addition of the IP agonist (Fig. 5*C*). In addition, the number of IFN-γ–producing cells was enhanced by the IP agonist in a dose-dependent manner when anti-CD3 Ab and anti-CD28 Ab were present at concentrations of 10 and 100 μg/ml, respectively (Fig. 5*D*). Moreover, the number of T-bet$^+$ cells was increased by the addition of 1 μg/ml iloprost under the Th1-skewing conditions in the presence of stimulation with 10 μg/ml anti-CD3 Ab and 100 μg/ml anti-CD28 Ab (Fig. 5*E*).

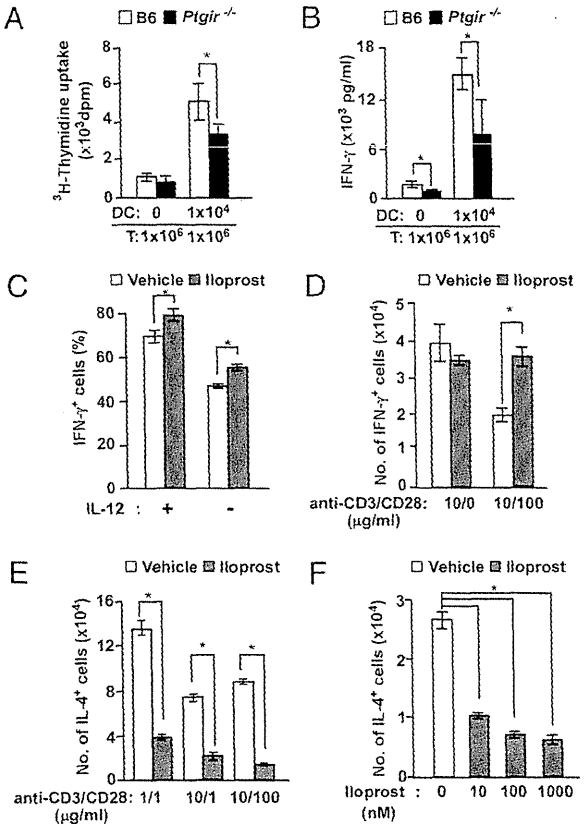

FIGURE 6. IP promotes Th1 differentiation but inhibits Th2 differentiation. *A* and *B*, MLR and cytokine production. Proliferation (*A*) and IFN-γ production (*B*) of CD4 T cells from B6 and *Ptgir*$^{-/-}$ mice was measured by [^{3}H]thymidine incorporation and ELISA ($n = 4$ per group). *C*, Effect of IP agonist on Th1/Tc1 and Th2 differentiation. CD4$^+$ T cells were incubated with or without IL-12 under Th1-skewing conditions in the presence or absence of iloprost, and the frequency of IFN-γ$^+$ cells is shown. *D*, Enhancement of Tc1 differentiation by IP stimulation. CD8$^+$ T cells from B6 mice were cultured under Th1/Tc1-skewing conditions with 1 μg/ml iloprost under plate-bound anti-CD3 (10 μg/ml) with or without CD28 (100 μg/ml) Abs. The numbers of IFN-γ$^+$ cells per well are shown. *E* and *F*, Th2 differentiation. Naive CD4$^+$ T cells from BALB/c mice were cultured under Th2-skewing condition in the presence or absence of 1 μg/ml iloprost with plate-bound anti-CD3 and CD28 Abs at the indicated concentrations (μg/ml) (*E*). In addition, naive CD4$^+$ T cells were cultured under Th2-skewing condition with plate-bound anti-CD3 (1 μg/ml) and CD28 (1 μg/ml) Abs in the presence or absence of iloprost at the indicated concentrations (ng/ml) (*F*). The numbers of IL-4$^+$ cells per well in triple wells are shown. Data are representative of three independent experiments with similar results. $*p < 0.05$ versus respective control values observed in the absence of each agonist.

We next evaluated the effect of endogenous PGI_2 production by DCs on T cell differentiation using an MLR assay. Alloreactive CD4$^+$ T cells were purified from B6 and *Ptgir*$^{-/-}$ mice and stimulated with DCs from BALB/c mice. Proliferation and IFN-γ production were inhibited in T cells from *Ptgir*$^{-/-}$ mice compared with T cells from B6 mice (Fig. 6*A*, 6*B*). Because the T cell proliferation and IFN-γ production stimulated with anti-CD3 and CD28 Abs were comparable between B6 and *Ptgir*$^{-/-}$ mice, the above results suggest that endogenous PGI_2 produced by DCs incites T cells to differentiate into Th1 cells. We further evaluated the possibility that Th1 differentiation is potentiated by IP signaling rather than by IL-12, a key inducer of Th1 differentiation. Even without IL-12 under the Th1-skewing conditions, the IP agonist increased the incidence of IFN-γ–producing cells (Fig. 6*C*). Similarly, Tc1 differentiation from CD8$^+$ cells was also enhanced by the IP agonist under the Th1/Tc1-skewing condition stimulated with strong CD28 engagement (Fig. 6*D*). These results indicate that PGI_2 facilitates Th1/Tc1 differentiation through its specific receptor, IP.

Because IL-4 was not detected in the culture supernatant of proliferating LN cells (Fig. 3*B*), presumably due to the genetic background of the mice used, it remained unclear whether Th2 differentiation is modulated by IP engagement. To clarify this issue, we prepared naive CD4$^+$ T cells from Th2-dominant BALB/c mice and incubated them under Th2-skewing conditions. In contrast to the above results regarding Th1, the addition of the IP agonist decreased the number of IL-4–producing cells under the Th2-skewing condition regardless of the degree of anti-CD28 engagement (Fig. 6*E*). Furthermore, iloprost yielded an inhibition of the generation of IL-4–producing cells in a dose-dependent manner (Fig. 6*F*). These

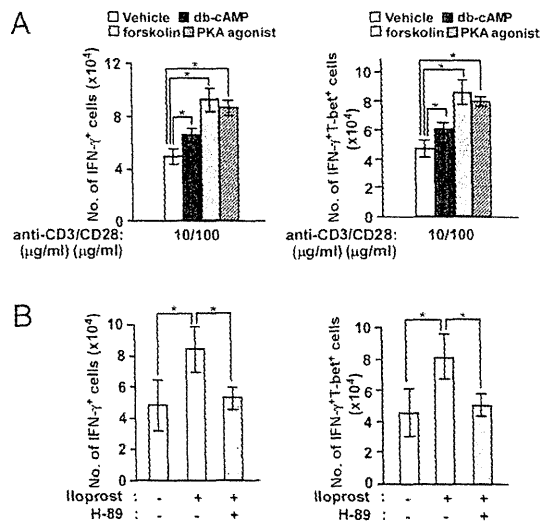

FIGURE 7. IP facilitates Th1 differentiation in vitro through the cAMP/PKA pathway. *A*, Effects of cAMP and PKA on Th1 differentiation. CD4$^+$ T cells from B6 mice were cultured under the Th1-skewing condition with or without 10 μM db-cAMP, 100 nM forskolin, and 100 μM N^6-Bnz-cAMP (a PKA agonist) with the indicated concentrations of plate-bound anti-CD3 and CD28 Abs. The numbers of IFN-γ$^+$ (*left panel*) and T-bet$^+$ cells (*right panel*) per well are shown. *B*, Effects of a PKA inhibitor on Th1 differentiation through iloprost. Under Th1-skewing condition with plate-bound anti-CD3 (10 μg/ml) and CD28 Abs (100 μg/ml), CD4$^+$ T cells from B6 mice were cultured with or without 1 μM of iloprost in the presence or absence of 3 μM H-89, a PKA inhibitor. The numbers of IFN-γ$^+$ (*left panel*) and T-bet$^+$ cells (*right panel*) per well are shown. Representative data from three independent experiments are shown. $*p <$ 0.05 between the indicated groups.

results suggest that IP activation facilitates Th1 differentiation but inhibits Th2 differentiation.

Facilitation of Th1 differentiation by IP signaling through cAMP-PKA signaling

Because it is known that IP mediates signaling via the elevation of cAMP and the activation of PKA as a downstream signal, we examined the involvement of cAMP/PKA signaling in the facilitation of Th1 differentiation. The addition of cAMP analogs db-cAMP and forskolin and a PKA agonist N^6-Bnz-cAMP to the Th1-skewing conditions increased the number of IFN-γ–producing cells and T-bet$^+$ cells under the engagement of anti-CD28 Ab (Fig. 7*A*). In addition, the induction of Th1 differentiation by the IP agonist was inhibited by treatment with H89, an inhibitor of PKA signaling (38) (Fig. 7*B*). These results suggest that the enhancement of Th1 differentiation induced by PGI$_2$-IP signaling is mediated through the induction of T-bet via the cAMP-PKA pathway.

Discussion

The effect of PGI$_2$-IP signaling on Th1 differentiation remains controversial. Using CHS as a representative Th1/Tc1-induced immune response, we have demonstrated that the CHS response is inhibited in *Ptgir*$^{-/-}$ mice. We have also found that PGIS and IP are present in DCs and T cells, respectively. In addition, an IP agonist enhanced Th1 differentiation under Th1-skewing conditions in vitro, and this enhancement was eliminated by a PKA inhibitor. These results suggest that PGI$_2$-IP signaling promotes Th1/Tc1 differentiation to induce CHS responses.

Thus far, with the exception of one paper claiming that Th17-mediated collagen-induced arthritis facilitated by IP signaling (39), there is wide agreement that IP has immunosuppressive effects. For example, IP has been reported to suppress asthma in mice through the inhibition of migration and maturation of DCs in vivo (24) and to inhibit both Th1 and Th2 cytokine production in vitro (23). Consistent with these findings, we found that DC functions in *Ptgir*$^{-/-}$ mice were somewhat enhanced and that an IP agonist suppressed Th1 differentiation in the absence of anti-CD28 Ab stimulation. In contrast, we found that the IP analog enhanced Th1 differentiation in the presence of anti-CD28 Ab stimulation. This observation is consistent with the finding that proliferation and IFN-γ production of IP-deficient T cells was inhibited compared with those of control T cells when stimulated with allogeneic DCs that produce PGI$_2$ (Fig. 7*A*, 7*B*). Because a PKA inhibitor eliminated the enhancement of Th1 differentiation by the IP agonist, this effect appears to be mediated through the cAMP-PKA pathway. Therefore, PGI$_2$-IP signaling seems to enhance Th1/Tc1 differentiation via the cAMP-PKA pathway under strong CD28 engagement, which agrees with our current in vivo findings, namely, that the Th1/Tc1-driven CHS response was inhibited in *Ptgir*$^{-/-}$ mice.

Because PGI$_2$ is very unstable in physiological conditions, understanding its mechanisms will require the identification of the cellular source of PGI$_2$ and the cells expressing IP. One candidate for the cellular source of PGI$_2$ is the DCs, which control T cell differentiation and form a close interface with T cells referred as the immunological synapse (40). The induction of PGI$_2$ is controlled by PGIS and COX-2, and we found that DCs produced a large amount of 6-keto PGF$_{1\alpha}$, a stable metabolite of PGI$_2$, in their culture supernatant. On the other hand, we detected IP in both T cells and DCs. On the other hand, we have demonstrated that IP signaling in T cells promotes Th1/Tc1 differentiation with the support of CD28 engagement. It is noteworthy that IP was mostly expressed by Th2 cells but much less in Th1 cells (25); therefore, IP-induced Th1/Tc1 differentiation most likely occurs at the initiation of T cell differentiation. The above findings, taken together with the previous reports, indicate that IP suppresses DCs functions but enhances Th1/Tc1 differentiation. This dual function of IP may serve to reveal the physiological role of PGI$_2$-IP signaling in various animal models.

The inhalation of IP agonists, such as iloprost, is a widely used treatment for pulmonary hypertension. Although it has been reported that iloprost inhibits human asthmatic responses by preventing bronchoconstriction (26, 27) and rhinorrhea (41), the immunological effects of PGI$_2$ in humans remain unclear. We have previously reported an increased IgE level in *Ptgir*$^{-/-}$ mice after repeated sensitization with OVA (42), which is consistent with our current data suggesting that PGI$_2$ suppresses Th2 differentiation of naive mouse T cells in vitro. Therefore, the PGI$_2$-IP signaling cascade might have an inhibitory effect on Th2-type immune diseases, such as atopic dermatitis and allergic asthma. Future studies will clarify how PGI$_2$ signaling operates in the human immune system and how it can be exploited to treat various immune diseases.

Disclosures

The authors have no financial conflicts of interest.

References

1. Liew, F. Y. 2002. T(H)1 and T(H)2 cells: a historical perspective. *Nat. Rev. Immunol.* 2: 55–60.
2. Mosmann, T. R., and S. Sad. 1996. The expanding universe of T-cell subsets: Th1, Th2 and more. *Immunol. Today* 17: 138–146.
3. Weaver, C. T., R. D. Hatton, P. R. Mangan, and L. E. Harrington. 2007. IL-17 family cytokines and the expanding diversity of effector T cell lineages. *Annu. Rev. Immunol.* 25: 821–852.
4. Badou, A., M. Savignac, M. Moreau, C. Leclerc, G. Foucras, G. Cassar, P. Paulet, D. Lagrange, P. Druet, J. C. Guéry, and L. Pelletier. 2001. Weak TCR stimulation induces a calcium signal that triggers IL-4 synthesis, stronger TCR stimulation induces MAP kinases that control IFN-gamma production. *Eur. J. Immunol.* 31: 2487–2496.
5. Constant, S. L., and K. Bottomly. 1997. Induction of Th1 and Th2 CD4+ T cell responses: the alternative approaches. *Annu. Rev. Immunol.* 15: 297–322.
6. Szabo, S. J., B. M. Sullivan, S. L. Peng, and L. H. Glimcher. 2003. Molecular mechanisms regulating Th1 immune responses. *Annu. Rev. Immunol.* 21: 713–758.
7. Kabashima, K., and Y. Miyachi. 2004. Prostanoids in the cutaneous immune response. *J. Dermatol. Sci.* 34: 177–184.
8. Matsuoka, T., and S. Narumiya. 2008. The roles of prostanoids in infection and sickness behaviors. *J. Infect. Chemother.* 14: 270–278.
9. Narumiya, S., Y. Sugimoto, and F. Ushikubi. 1999. Prostanoid receptors: structures, properties, and functions. *Physiol. Rev.* 79: 1193–1226.
10. Goodwin, J. S., and J. Ceuppens. 1983. Regulation of the immune response by prostaglandins. *J. Clin. Immunol.* 3: 295–315.
11. Hasler, F., H. G. Bluestein, N. J. Zvaifler, and L. B. Epstein. 1983. Analysis of the defects responsible for the impaired regulation of EBV-induced B cell proliferation by rheumatoid arthritis lymphocytes. II. Role of monocytes and the increased sensitivity of rheumatoid arthritis lymphocytes to prostaglandin E. *J. Immunol.* 131: 768–772.
12. Betz, M., and B. S. Fox. 1991. Prostaglandin E2 inhibits production of Th1 lymphokines but not of Th2 lymphokines. *J. Immunol.* 146: 108–113.
13. Nataraj, C., D. W. Thomas, S. L. Tilley, M. T. Nguyen, R. Mannon, B. H. Koller, and T. M. Coffman. 2001. Receptors for prostaglandin E(2) that regulate cellular immune responses in the mouse. *J. Clin. Invest.* 108: 1229–1235.
14. Kabashima, K., T. Saji, T. Murata, M. Nagamachi, T. Matsuoka, E. Segi, K. Tsuboi, Y. Sugimoto, T. Kobayashi, Y. Miyachi, et al. 2002. The prostaglandin receptor EP4 suppresses colitis, mucosal damage and CD4 cell activation in the gut. *J. Clin. Invest.* 109: 883–893.
15. Nagamachi, M., D. Sakata, K. Kabashima, T. Furuyashiki, T. Murata, E. Segi-Nishida, K. Soontrapa, T. Matsuoka, Y. Miyachi, and S. Narumiya. 2007. Facilitation of Th1-mediated immune response by prostaglandin E receptor EP1. *J. Exp. Med.* 204: 2865–2874.
16. Yao, C., D. Sakata, Y. Esaki, Y. Li, T. Matsuoka, K. Kuroiwa, Y. Sugimoto, and S. Narumiya. 2009. Prostaglandin E(2)-EP4 signaling promotes immune inflammation through T(H)1 cell differentiation and T(H)17 cell expansion. *Nat Med.* 15: 633–640.
17. Lee, I. Y., Y. D. Bae, D. I. Jeoung, D. Kang, C. H. Park, S. H. Kim, and J. Choe. 2007. Prostacyclin production is not controlled by prostacyclin synthase but by cyclooxygenase-2 in a human follicular dendritic cell line, HK. *Mol. Immunol.* 44: 3168–3172.
18. Sugimoto, M., I. Arai, N. Futaki, Y. Hashimoto, T. Sakurai, Y. Honma, and S. Nakaike. 2006. Time course changes of scratching counts, dermatitis